PHOTOCHEMISTRY OF $Fe_2(CO)_8(\mu\text{-}CH_2)$

A THESIS

Presented in Partial Fulfillment of the Requirements for

the Degree of Master of Science in the

Graduate School of The Ohio State University

By

Daniel M. Branan, B.S.

*****

The Ohio State University
1997

Master's Examination Committee:

Dr. Bruce E. Bursten, Advisor

Dr. Andrew Wojcicki

Approved By

Bruce E Bursten

Advisor
Department of Chemistry

REPORT DOCUMENTATION PAGE

Form Approved
OMB No. 0704-0188

1. AGENCY USE ONLY *(Leave blank)*	2. REPORT DATE	3. REPORT TYPE AND DATES COVERED
	12 Dec 96	

4. TITLE AND SUBTITLE

Photochemistry of $Fe_2(CO)_8(\mu\text{-}CH_2)$

5. FUNDING NUMBERS

6. AUTHOR(S)

Daniel M. Branan

7. PERFORMING ORGANIZATION NAME(S) AND ADDRESS(ES)

Ohio State University

8. PERFORMING ORGANIZATION REPORT NUMBER

96-096

9. SPONSORING / MONITORING AGENCY NAME(S) AND ADDRESS(ES)

DEPARTMENT OF THE AIR FORCE
AIR FORCE INSTITUTE OF TECHNOLOGY/CI
2950 P STREET
WRIGHT-PATTERSON AFB OH 45433-7765

10. SPONSORING / MONITORING AGENCY REPORT NUMBER

11. SUPPLEMENTARY NOTES

12a. DISTRIBUTION / AVAILABILITY STATEMENT

Unlimited

12b. DISTRIBUTION CODE

13. ABSTRACT *(Maximum 200 words)*

14. SUBJECT TERMS

15. NUMBER OF PAGES

59

16. PRICE CODE

17. SECURITY CLASSIFICATION OF REPORT	18. SECURITY CLASSIFICATION OF THIS PAGE	19. SECURITY CLASSIFICATION OF ABSTRACT	20. LIMITATION OF ABSTRACT

GENERAL INSTRUCTIONS FOR COMPLETING SF 298

The Report Documentation Page (RDP) is used in announcing and cataloging reports. It is important that this information be consistent with the rest of the report, particularly the cover and title page. Instructions for filling in each block of the form follow. It is important to ***stay within the lines*** to meet ***optical scanning requirements***.

Block 1. Agency Use Only *(Leave blank)*.

Block 2. Report Date. Full publication date including day, month, and year, if available (e.g. 1 Jan 88). Must cite at least the year.

Block 3. Type of Report and Dates Covered. State whether report is interim, final, etc. If applicable, enter inclusive report dates (e.g. 10 Jun 87 - 30 Jun 88).

Block 4. Title and Subtitle. A title is taken from the part of the report that provides the most meaningful and complete information. When a report is prepared in more than one volume, repeat the primary title, add volume number, and include subtitle for the specific volume. On classified documents enter the title classification in parentheses.

Block 5. Funding Numbers. To include contract and grant numbers; may include program element number(s), project number(s), task number(s), and work unit number(s). Use the following labels:

C	- Contract	**PR**	- Project
G	- Grant	**TA**	- Task
PE	- Program Element	**WU**	- Work Unit Accession No.

Block 6. Author(s). Name(s) of person(s) responsible for writing the report, performing the research, or credited with the content of the report. If editor or compiler, this should follow the name(s).

Block 7. Performing Organization Name(s) and Address(es). Self-explanatory.

Block 8. Performing Organization Report Number. Enter the unique alphanumeric report number(s) assigned by the organization performing the report.

Block 9. Sponsoring/Monitoring Agency Name(s) and Address(es). Self-explanatory.

Block 10. Sponsoring/Monitoring Agency Report Number. *(If known)*

Block 11. Supplementary Notes. Enter information not included elsewhere such as: Prepared in cooperation with...; Trans. of...; To be published in.... When a report is revised, include a statement whether the new report supersedes or supplements the older report.

Block 12a. Distribution/Availability Statement. Denotes public availability or limitations. Cite any availability to the public. Enter additional limitations or special markings in all capitals (e.g. NOFORN, REL, ITAR).

- **DOD** - See DoDD 5230.24, "Distribution Statements on Technical Documents."
- **DOE** - See authorities.
- **NASA** - See Handbook NHB 2200.2.
- **NTIS** - Leave blank.

Block 12b. Distribution Code.

- **DOD** - Leave blank.
- **DOE** - Enter DOE distribution categories from the Standard Distribution for Unclassified Scientific and Technical Reports.
- **NASA** - Leave blank.
- **NTIS** - Leave blank.

Block 13. Abstract. Include a brief *(Maximum 200 words)* factual summary of the most significant information contained in the report.

Block 14. Subject Terms. Keywords or phrases identifying major subjects in the report.

Block 15. Number of Pages. Enter the total number of pages.

Block 16. Price Code. Enter appropriate price code *(NTIS only)*.

Blocks 17. - 19. Security Classifications. Self-explanatory. Enter U.S. Security Classification in accordance with U.S. Security Regulations (i.e., UNCLASSIFIED). If form contains classified information, stamp classification on the top and bottom of the page.

Block 20. Limitation of Abstract. This block must be completed to assign a limitation to the abstract. Enter either UL (unlimited) or SAR (same as report). An entry in this block is necessary if the abstract is to be limited. If blank, the abstract is assumed to be unlimited.

★U.S.GPO:1993-0-336-043

PHOTOCHEMISTRY OF $Fe_2(CO)_8(\mu\text{-}CH_2)$

By

Daniel M. Branan, M.S.

The Ohio State University, 1997

Professor Bruce E. Bursten, Advisor

We herein present the previously unreported photochemistry of two forms of the dimetallocyclopropane complex $Fe_2(CO)_8(\mu\text{–}CH_2)$, and its deuterated analog. We have determined that it behaves similarly to other dimetallic carbonyls in that it eliminates carbon monoxide upon irradiation with high-intensity UV/visible light to form distinct single and double CO-loss products. Upon formation of a 34-electron single CO-loss product, however, it exhibits the ability to either maintain an unbalanced 16/18-electron configuration, or convert to a carbene complex with an iron-iron double bond. This unusual behavior is possibly due to the high degree of π-interaction between the $\mu\text{-}CH_2$ ligand and the dimetallic center. There is also evidence that a *solvento* compound is being formed which could explain both the stability of the single CO-loss product and the apparent formation of $Fe(CO)_5$ within the low-temperature matrix.

ABSTRACT

We herein present the previously unreported photochemistry of two forms of the dimetallocyclopropane complex $Fe_2(CO)_8(\mu\text{–}CH_2)$, and its deuterated analog. We have determined that it behaves similarly to other dimetallic carbonyls in that it eliminates carbon monoxide upon irradiation with high-intensity UV/visible light to form distinct single and double CO-loss products. Upon formation of a 34-electron single CO-loss product, however, it exhibits the ability to either maintain an unbalanced 16/18-electron configuration, or convert to a carbene complex with an iron-iron double bond. This unusual behavior is possibly due to the high degree of π-interaction between the μ-CH_2 ligand and the dimetallic center. There is also evidence that a *solvento* compound is being formed which could explain both the stability of the single CO-loss product and the apparent formation of $Fe(CO)_5$ within the low-temperature matrix.

DEDICATION

To my loving and supportive wife Tammy, without whose help I could never have embarked upon nor successfully completed this venture.

ACKNOWLEDGMENTS

I wish to thank my advisor, Dr. Bruce E. Bursten, and the members of his research group, for their gracious acceptance and untiring assistance during my education at The Ohio State University. Many thanks, especially, to Dr. Marcello Vitale, whose broad knowledge-base and astute questions aided my research on more than one occasion.

I also wish to thank my undergraduate advisor, Dr. Norris W. Hoffman, for allowing me to experience laboratory research at an early point in my career, and for going above and beyond the call of duty in support of my pursuit of a post-graduate education.

Finally, I thank Dr. Nathan C. Miller, who, through a single piece of advice, aided me more than he will ever know in my search for a fulfilling career.

VITA

February 17, 1966	Born - Milwaukee, WI
1988	B.S., Chemistry University of South Alabama
1995 - Present	Graduate Student The Ohio State University

PUBLICATIONS

1. Branan, D. M.; Hoffman, N. W.; McElroy, E. A.; Prokopuk, N.; Salazar, A. B.; Robbins, M. J.; Hill, W. E.; Webb, T. R., "Synthesis and reactivity of carbonylbis(triphenylphosphine)rhodium(I) complexes of water and weakly coordinating anions", *Inorganic Chemistry*, 30(6), 1200, (1991)

2. Branan, D. M.; Hoffman, N. W.; McElroy, E. A.; Ramage, D. L.; Robbins, M. J.; Eyler, J. R.; Watson, C. H.; DeFur, P.; Leary, J. A., "Comparison of laser-desorption and fast-atom bombardment mass spectra of a series of rhodium $Rh(PPh_3)_2(CO)Y$ complexes", *Inorganic Chemistry*, 29(10), 1915, (1990)

3. Araghizadeh, F.; Branan, D. M.; Hoffman, N. W.; Jones, J. H.; McElroy, E. A.; Miller, N. C.; Ramage, D. L.; Salazar, A. B.; Young, S. H., "Relative affinities of carbonylbis(triphenylphosphine)rhodium(I) and related cations fo anionic ligands in dichloromethane", *Inorganic Chemistry*, 27(21), 3752, (1988)

4. Branan, D. M.; Hoffman, N. W.; Jones, J. H.; McElroy, E. A.; Miller, N. C.; Ramage, D. L.; Schott, A. F.; Young, S. H., "Anion affinity of carbonylbis(triphenylphosphine)rhodium(I) in dichloromethane: fluoride vs. its halide analogs", *Inorganic Chemistry*, 26(17), 2915, (1987)

FIELDS OF STUDY

Major Field: Chemistry

TABLE OF CONTENTS

LIST OF TABLES

LIST OF FIGURES

INTRODUCTION

"Knowledge is of two kinds. We know a subject ourselves, or we know where we can find information upon it."

Samuel Johnson

Matrix Photochemistry

The photochemical activity of metal carbonyl complexes has been a subject of interest since the discovery of metal carbonyls themselves. Only one year after Ludwig Mond's history-making discovery of $Ni(CO)_4$, he published the observation that $Fe(CO)_5$ reacted photochemically to produce carbon monoxide and the stable dinuclear compound $Fe_2(CO)_9$.[1] More recently, dinuclear systems of various types have been successfully studied, yielding a great deal of new information about CO-loss chemistry and metal-metal bonding.[2] The study of photochemistry is greatly aided by isolating the molecules of interest in some manner, so their behavior may be observed on a reasonable time-scale. There are many different ways of doing this, but we will only employ one of them. The isolating "matrix" in this case will be a frozen hydrocarbon matrix, and the behaviors of interest are the structural changes which take place upon the photochemical liberation of carbon monoxide. This thesis reports the investigation of the photochemistry of the dimetallocyclopropane complex $Fe_2(CO)_8(\mu\text{-}CH_2)$ (**1**).

A Brief Discussion of Dimetallocyclopropanes

Dimetallocyclopropanes are a relatively new entry in the field of organometallic chemistry, with the first recognized synthesis of such a compound having occurred a mere twenty-one years ago[3]. However, these unique complexes have sparked the interest of a wide range of chemists, from those investigating the behavior of carbenes at metal interfaces, to those developing molecular carbon monoxide sensors[4]. Indeed, the methylene bridge is a remarkable entity, and lends surprising stability to the complexes in which it is found. Generally, dimetallocyclopropanes are soluble in a wide variety of organic solvents, are quite insensitive to both oxygen and moisture, and are usually intensely colored[3]. The source of this stabilizing effect is the excellent π-backbonding nature of the methylene bridge,[3,5,6] a facet of the ligand that was not initially recognized. In fact, the amount of π overlap between μ-CH_2 and a dimetallic center has been shown to be almost 30% greater than for CO. Combined with its considerable σ overlap, the bond energy of μ-CH_2 in a dimetallocyclopropane is calculated to be over 260% stronger than a similarly bound μ–CO! [7]

An excellent example of this effect is in the case of $Os_2(CO)_9$ and $Os_2(CO)_8(\mu$-$CH_2)$. Diosmium enneacarbonyl is more properly formulated as $Os_2(CO)_8(\mu$-CO), since it exists as such in both crystalline form and solution, and possesses C_{2v} symmetry. It is extremely unstable, requiring synthesis temperatures of <233 K, and decomposing rapidly in solution[8]. However, the mere replacement (symbolically) of one carbonyl oxygen with two hydrogens results in an air-stable diosmacyclopropane that can be synthesized at standard temperatures and pressures[9]!

The analogous transformation of $Fe_2(CO)_9$ is not as evident, but is nonetheless remarkable. With iron being a much smaller molecule than osmium, the carbonyls bridge more readily, resulting in a highly symmetric (D_{3h}) triply-bridged complex. Once again, the replacement of μ-CO with μ-CH_2 significantly changes the molecular properties. Suddenly, a substance which was virtually insoluble in all solvents, becomes a substance that is soluble and stable in almost any organic solvent. Even though $Fe_2(CO)_9$ *appears* to be quite stable, and indeed is much more so than the Os analogue, this is only due to the fact that it is sparingly soluble in the majority of solvents. Once it is in solution, in any solvent except for $Fe(CO)_5$, it becomes quite unstable and decomposes into $Fe(CO)_5$ and $Fe(CO)_4$[solv]. Even under relatively mild conditions, chemical reactions of $Fe_2(CO)_9$ frequently result in significant amounts of mono-metallic products[10,11,12]. Contrastingly, $Fe_2(CO)_8(\mu\text{-}CH_2)$ is extremely stable in solution. Even under fairly rigorous thermal conditions, such as in refluxing benzene for several hours, the metal-metal bond remains intact.

A Literature Review of $Fe_2(CO)_8(\mu\text{-}CH_2)$, 1979 to Present

In the Fall of 1979, a communication from the research group of the late Dr. Rowland Pettit (University of Texas, Austin) was received at the offices of the Journal of the American Chemical Society. The subject was the synthesis of the "novel organometallic complex," $Fe_2(CO)_8(\mu\text{-}CH_2)$[13]. Between this initial communication, the follow-up article[28], and an additional paper from Meyer, Riley and Davis[14] (both published in 1982) the physical characteristics of this complex were fully described. This

characterization included infrared, nuclear magnetic resonance, and Mössbauer spectroscopies, and X-ray crystallography. It was shown to have a crystalline structure similar to that of $Fe_2(CO)_9$ (Figure 1), with a singly-bridged structure (Figure 2) predominating almost exclusively in solution[28]. Additionally, **1** was demonstrated to react with an H_2/CO mixture to produce methane, as in the Fischer-Tropsch Process. This reactivity, and its relatively simple structure, immediately made **1** the leading candidate for a model of the "surface-bound methylene" mechanism for the Fischer-Tropsch Process. As alluded to in the previous section, the bonding of the CH_2 moiety was not fully understood at the time, and it was initially thought to be sp^3 hybridized[14]. However, interleaved between the output from the University of Texas was a short communication published by Vites and Fehlner in the *Journal of Electronic Spectroscopy and Related Phenomena.* This article reported the first photoelectron (PE) spectroscopic treatment of **1**.[5] The results obtained led the authors to make three conclusions that were significant to understanding the bonding characteristics of the methylene bridge:

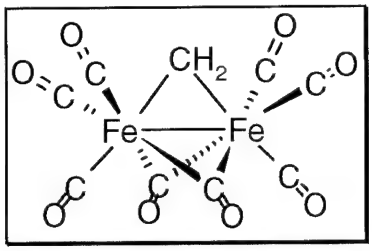

Figure 1 - Triply-Bridged Structure of $Fe_2(CO)_8(\mu\text{-}CH_2)$

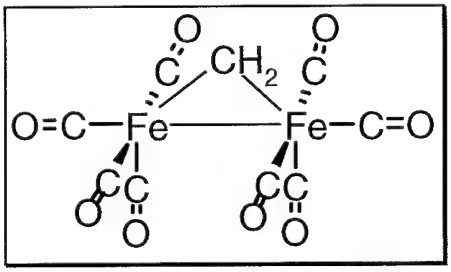

Figure 2 - Singly-Bridged Structure of $Fe_2(CO)_8(\mu\text{-}CH_2)$

1) The $\mu\text{-}CH_2$ ligand retained a relatively high negative charge, in agreement with current theoretical results.

2) The $1b_1$ orbital of μ-CH_2 (Figure 4) had a low enough energy to interact with, and allow donation of electron density from, the HOMO of the Fe-Fe fragment (Figure 3).

3) The bonding in **1** was strictly analogous to the bonding in cyclopropane, further legitimizing the "dimetallocyclopropane" label.

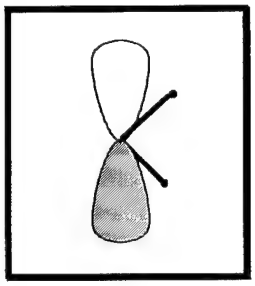

Figure 4 - $1b_1$ Orbital of μ-CH_2

In 1982, a second PE spectroscopic treatment was reported by Xiang, *et al.* which confirmed the findings of Vites and Fehlner. Additionally, they reported the carbon 1s and oxygen 1s core binding energies, and calculated the charge on the methylene to be a substantial -0.5 ± 0.2 [15].

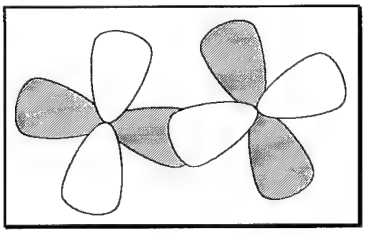

Figure 3 - HOMO of the Fe-Fe Fragment

After a four year silence, **1** appeared once again as the subject of a major publication. Chang, *et al.* reported the first cryogenic matrix isolation study of **1**, with the emphasis being placed on the methylene bridge itself. Based upon the calculated H-C-H bond angle of 106°, and the ^{13}C NMR coupling constant of 147 Hz, the authors concluded that the methylene carbon was indeed sp^3 hybridized[30]. This, of course, was in direct opposition to the earlier findings regarding the π-accepting ability of μ-CH_2, since an sp^3-hybridized carbon would have no available 2p orbital. However, the "last word" on this controversy, at least chronologically, appeared in a 1993 publication in *Spectrochimica Acta.* In this excellent paper, the IR frequencies and intensities of C-H vibrational modes were analyzed

for twelve different organometallic systems, including **1**.[6] This Italian-German team of seven scientists reached the same conclusion as the PE spectroscopists had several years earlier, but for a more general case. Namely, they concluded that M_n-$CH_{(4-n)}$ systems exhibit "the unexpected presence of an opposite π-effect, which increases as n increases." (*ibid.*, p. 1258)

The remainder of the publications in which **1** appears, from 1986 to present, can be divided into two classes. The first class refers to **1** as a building-block in the creation of more complex systems, especially heterogenous metal carbonyl clusters.[4,16,17,18,19,20] The second class represents those publications that reference **1** as a model for some reaction mechanism featuring a metal-bound methylene intermediate.[21,22,23,24,25] Indeed, this "novel organometallic complex", as represented by the original communication and following article, has lived a remarkably useful life in the literature to date. Taken together, these publications have been cited a total of 161 times, averaging more than 9 citations *per annum*.[26]

The $Fe_2(CO)_8(\mu\text{-}CH_2)$ Molecule

General Discussion

As indicated above, a fair amount of physical data has been collected for this molecule. For the purposes of this thesis, however, only the IR and NMR data is pertinent. These data have been compiled in Table 1.

Type of Spectroscopy	Solvent	Units	Peak Values	Ref
Infrared	hexanes	ν-CO, cm^{-1}	2118(w), 2058(vs), 2028(vs), 2012(s)	28
	C_5Cl_6 (mull)	ν-CO, cm^{-1}	2916(w), 2072(m), 2020(s), 1875(sh), 1836(s)	
	Ar (12 K)	ν-CH_2, cm^{-1}	2975.0, 2925.0, 978, 936.5, 759.8	30
	N_2 (12 K)	ν-CH_2, cm^{-1}	2981.2, 2933.2, 974.4, 932.8, 764.6	30
	Ar (12 K)	ν-CD_2, cm^{-1}	2235.8, 2152.9, 754.5, 723.7, 627.7, 543.8	30
	N_2 (12 K)	ν-CD_2, cm^{-1}	2243.5, 2157.2, 752.1, 725.0, 626.8, 545.0	30
^{1}H NMR	acetone-d_6	δ	5.5(s)	28

Table 1 - Spectroscopic Data from the Literature

In the "flagship" 1982 publication from the Pettit group, several derivatives of **1** were synthesized, and a large number of thermal reactions were studied. Besides the aforementioned reaction with H_2 to produce methane and acetaldehyde, **1** was also found to react with short-chain olefins, such as ethylene and propylene, to give one-carbon homologation products. Treatment with ethylene (400 p.s.i.) resulted in >90% production of propylene. Treatment with propylene gave mostly isobutylene, along with small amounts of *cis*- and *trans*- 2-butene and *n*-butene. The general conclusion was reached that the loss of CO preceded the chemical reaction, since these reactions were inhibited by the presence of CO gas. The reactions were assumed to proceed through the nucleophilic attack of either the hydrogen or the π complex on a coordinatively unsaturated iron after the loss of a CO ligand. This was presumed to lead to incorporation of the μ-CH_2 into an expanded metallocycle, with β-hydride elimination producing an elongated π complex coordinated to one of the irons, and reductive elimination producing the observed products. An interesting theoretical study published in 1985 took issue with the above

mechanism by studying the energies of the molecular orbitals involved in two possible mechanisms. One of these was Pettit's mechanism, and the other was one proposed by the authors in which the metallocyclopropane ring opened to allow nucleophilic attack at the methylene[27]. The authors concluded that Pettit's mechanism was energetically unfavorable, but did not attempt to explain the observed inhibition due to CO pressure.

Photochemistry

Simply put, no study of the photochemistry of **1** currently exists in the literature. The interest in **1** has historically, and understandably, revolved around the methylene bridge. Consequently, a part of this molecule that normally enjoys a great deal of attention has been rigorously ignored -- the carbonyls. Even in Chang's excellent infrared matrix isolation analysis, the carbonyl peaks are relegated to the additional material[30]. If, in fact, CO-loss is an integral part of the reactivity of **1**, it would seem that the study of photochemical CO-loss products would be particularly useful. As noted above, **1** is known to exist in solution with only terminal CO ligands, and is assumed to possess C_{2v} symmetry as shown in Figure 2. If this is the case, it would have eight C-O stretching modes, seven of which would be IR-active (Figure 5). Of course, some of these modes may not possess the intensity to be detectable in a normal IR spectrum.

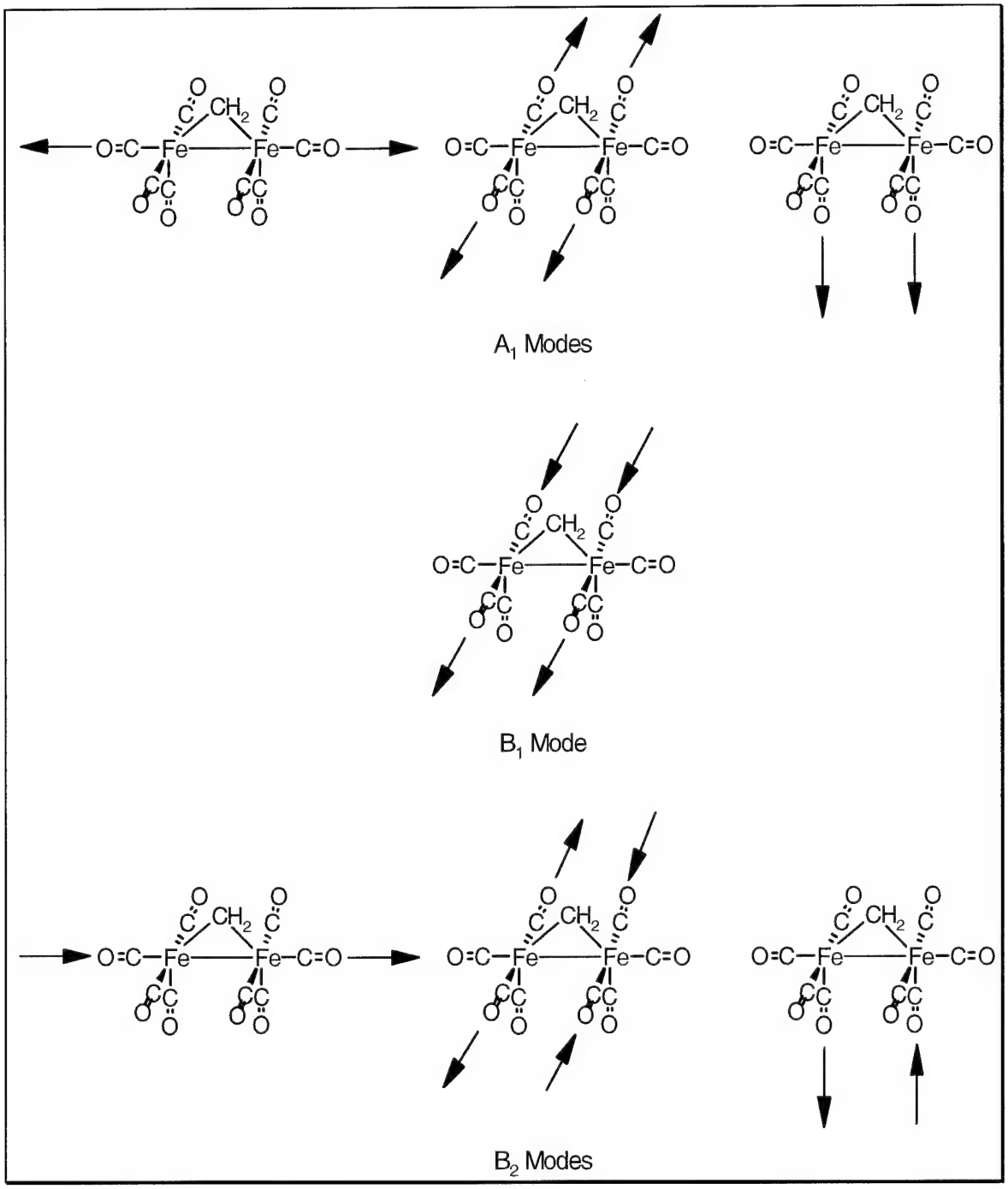

Figure 5 - IR-Active Carbonyl Stretching Modes of $Fe_2(CO)_8(\mu\text{-}CH_2)$

The Scope of this Thesis

In this thesis, we will study the UV-photochemistry of two molecules, **1** and its deuterated analogue $Fe_2(CO)_8(\mu\text{-}CD_2)$ (**2**). We will accomplish this by monitoring both the C-O and C-D stretching regions of the infrared spectrum, as well as utilizing nuclear magnetic resonance (NMR) and ultraviolet-visible (UV-Vis) spectroscopy. In so doing, we will attempt to answer the following questions:

- What is/are the photochemical CO-loss product(s)?
- Given the unusual strength of the $\mu\text{-}CH_2$ bonding, does the methylene bridge remain intact during the CO-loss process?
- How does the photochemistry of **1** relate to that of other metal-carbonyl complexes?

EXPERIMENTAL

"What mighty contests rise from trivial things."

Alexander Pope

General Laboratory Technique and Equipment

Air Sensitive Compounds

All reactions and manipulations of air-sensitive compounds were carried out under an atmosphere of Ar using standard procedures. The Ar (Linde) was additionally purified by passage through two consecutive columns containing activated De-Ox catalyst (Johnson and Matthey) and Drierite, respectively. Air-sensitive solids were handled and transferred in a Braun MB 150 M inert-atmosphere box ("dry-box") equipped with a BASF R3-11 catalyst/Linde 13x molecular sieve system. The atmosphere in the dry-box was maintained by periodic purging and regeneration of the catalyst. A titanocene chloride/zinc indicator was used to determine the state of the atmosphere. The catalyst was regenerated once each academic quarter, or whenever the titanocene indicator changed color. Evacuation of the access chambers and the dry-box itself was accomplished by a Leybold TRIVAC B rotary vane vacuum pump, which was capable of maintaining a pressure of 10^{-3} mbar. Compounds that were extremely air or moisture sensitive, or which posed a significant potential health risk, were stored in an Innovative

Technologies freezer which was integral to the dry-box itself.

Glassware

Routine glassware was washed thoroughly, rinsed three times with deionized water and dried in an oven. Volumetric glassware was washed with Aqua Regia, rinsed with deionized water until neutral, and kept in a 130 °C oven. When removed from the oven for use, the volumetric glassware was cooled under dynamic vacuum (-1000 mbar) to avoid water adsorption during the cooling process. Syringes with ground-glass plungers (Popper Micro-Mate®) were used for transferring larger volumes of liquid. When it was necessary to avoid air contact, these syringes were flushed three times with Ar before use. Hamilton gas-tight syringes were used for smaller, more accurate measurements. These were also flushed with Ar before use.

Infrared Spectrophotometry

A Nicolet FT-IR Magna-550 infrared spectrometer was used for acquiring infrared spectra. Typical spectra were collected at 1 or 2 cm^{-1} resolution for 32 scans. The liquid cell used for routine solution samples consisted of 20 x 10 mm NaCl plates with a 0.2 mm Teflon spacer, LuerLock ports, and Teflon plugs.

A specialized cell, manufactured by Specac, Inc., was used to collect the low-temperature spectra. This cell had a steel frame, CaF_2 windows, and a 1 mm path length. For data collection, the cell was mounted in a nickel-plated brass clamp at the end of a steel dewar (item 16, Figure 7). This entire assembly was placed inside a steel jacket

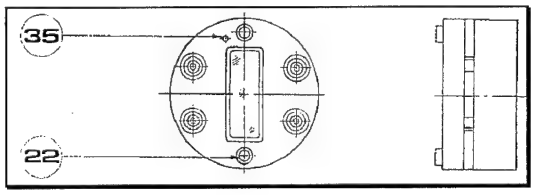

Figure 6 - Low-Temperature IR Cell

(item 2, Figure 7) and a vacuum pump was used to evacuate the cavity around the cell. The purpose of this was to eliminate anything that might condense on the cell windows at low temperatures (~100 K). To effect cooling, liquid N_2 was poured into the dewar. The temperature of the brass clamp was monitored with a thermocouple mounted inside the steel jacket. Another thermocouple monitored the temperature of the CaF_2 windows in the outer jacket. Both of these devices were connected to a controller which reported the approximate cell temperature and maintained the temperature of the outer windows (item 15, Figure 7) at approximately 30 °C. The controller could also warm the cell, but this was almost never used in order to avoid unnecessary thermal stress on the cell windows.

Our research group added an additional item to the cell which had the intended purpose of reducing thermal stress during the cooling phase. This was a copper shroud that was mounted on two sides of the brass cell clamp and extended to cover the entire length of the cell. The shroud only made physical contact with the clamp itself, and Indium spacers were used to ensure good thermal conductivity at these junctions. The sample was added with a Luer-lock adapter, which was threaded into the cell (item 22, Figure 6). This was typically done inside the dry-box to ensure there was no contamination from oxygen or moisture. The cell was washed with CH_2Cl_2 and dried under vacuum between samples.

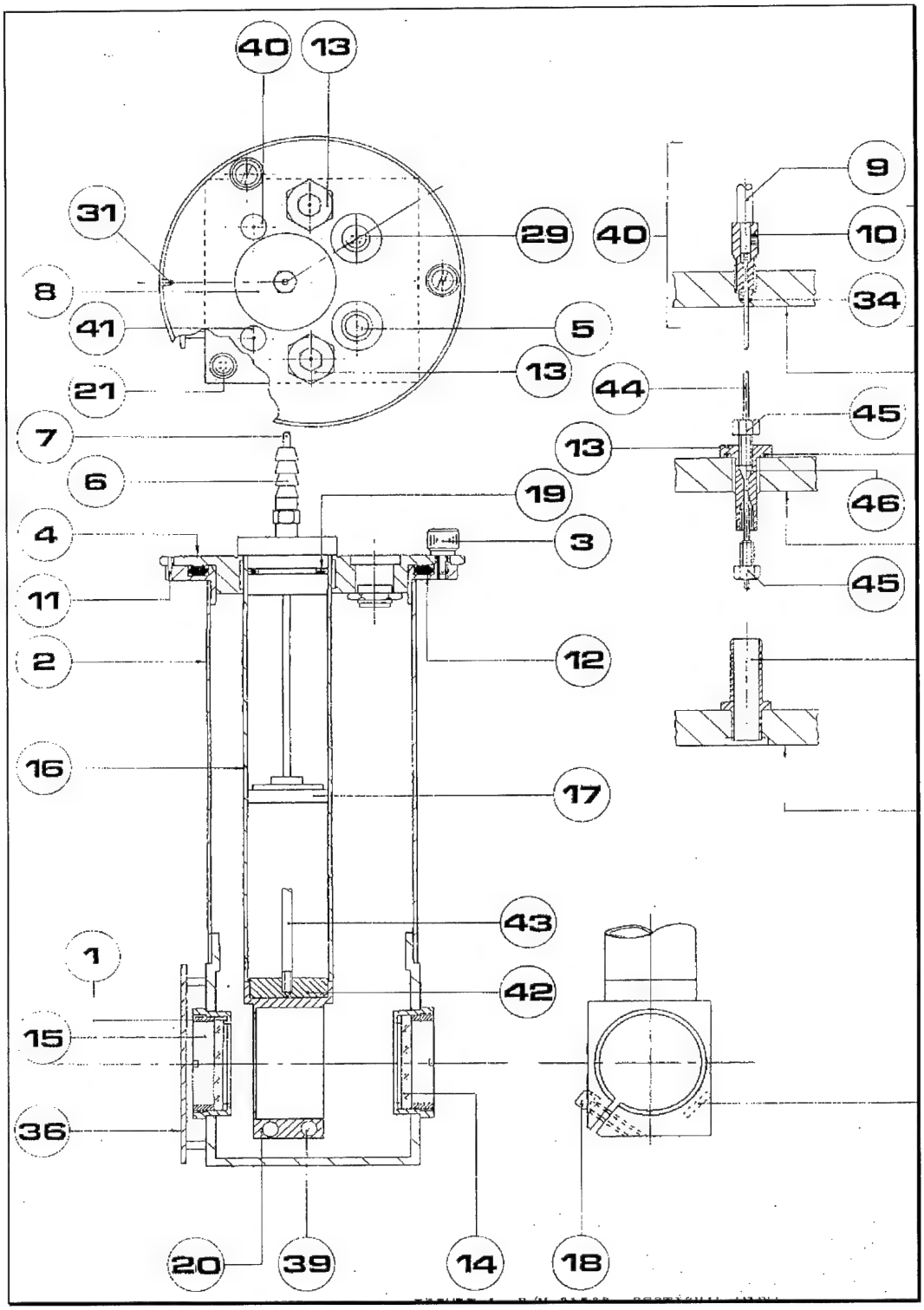

Figure 7 - Low Temperature IR Cell and Dewar

UV-Vis Spectrophotometry

A Cary-17I instrument, with a data acquisition and control upgrade by On Line Instrumentation Systems, Inc. (*OLIS*), was used to generate all UV-Vis spectra. Typical spectra were obtained using the low UV lamp setting. The OLIS-17 software resided on a "486" personal computer. One scan took approximately ten minutes and consisted of 16 observations per data point, with one data point per nm. Spectra were typically obtained between 800 and 250 nm in hydrocarbon solvents such as methylcyclohexane and 3-methylpentane.

The low-temperature IR cell described above was used for UV-Vis data collection also. A special tray was manufactured, which allowed it to be placed into the Cary-17I at an appropriate and reproducible location. Because the dewar was taller than the cavity in the machine, the cover that was usually placed over the top of the instrument could not be used. Instead, thick black felt material was placed around the top of the dewar in order to exclude external light.

Nuclear Magnetic Resonance (NMR) Spectroscopy

The NMR spectrometers we used were part of the Shared Analytical Instrumentation Laboratory of the OSU Department of Chemistry. The only spectra obtained for this work were proton (^{1}H) using the 200 MHz Bruker WP-200. Spectra were stored on the NMR computer, and hardcopies of each were produced.

Reagents and Solvents

With the exception of CD_2I_2, which was purchased from Cambridge Isotopes, all reagents were obtained through Aldrich. The $Fe(CO)_5$, Na, and CH_2I_2 or CD_2I_2 were used as purchased, without further purification. With the exception of Na, these were all purged with argon, sealed, and stored in a refrigerator. The sodium was stored under mineral oil and handled in the dry-box in order to preclude oxidation. The naphthalene was sublimed before use and stored under Ar. The $(C_2H_5)_4NBr$ was dried by heating it to 80 °C under dynamic vacuum overnight, and then stored under Ar.

Solvents were dried and degassed using standard methods. Most of the solvents were distilled over the appropriate drying agent, and collected under Ar for immediate use. The matrix solvents, 3-methylpentane (Aldrich, 3-MP) and methylcyclohexane (Aldrich) were stirred for at least twenty-four hours over a sodium-potassium alloy (NaK) to ensure complete dryness. Tetrahydrofuran (Mallinckrodt Analytical Reagent), THF, was dried and distilled from potassium/benzophenone. Hexanes (Mallinckrodt Analytical Reagent) were washed three times with concentrated sulfuric acid and subsequently washed with distilled water until neutral by Hydrion paper. The hexanes were then pre-dried over $MgSO_4$ and distilled over potassium metal. Acetone (Mallinckrodt Analytical Reagent) was distilled twice over fresh Drierite® and then refluxed continuously over activated molecular sieves (Advanced Specialty Gas Equipment, 4Å). Diethyl ether (Mallinckrodt Analytical Reagent) and absolute ethanol (AAPER Alcohol and Chemical Co.) were used as received, without additional drying or purification. Deionized water

from laboratory supply lines was degassed by bubbling Ar vigorously through it for at least 24 hours. This was used in lieu of distilled water.

Preparation of Compounds

As mentioned in the introductory section of this thesis, we confined our experimental efforts to compounds **1**, and **2**. A large sample of **1** was provided by Dr. Wojcicki's research group, having been prepared by Dr. Sarla Goel. We prepared small quantities of both these compounds by the method of Sumner, Collier and Pettit[28]. Both **1** and **2** are extremely air and moisture-stable and require no special handling after preparation.

$[Fe_2(CO)_8][(C_2H_5)_4N]_2$

This material was used subsequently to prepare both **1** and **2**. In the dry-box, Na (1.366 g , 0.059 mol) was weighed into a 100 mL Schlenk flask. The flask was removed from the dry-box and approximately 50 mL dry THF was needle-transferred under Ar. Naphthalene (0.652 g, 0.005 mol) was added while maintaining positive Argon flow through the flask. A pressure-equalizing dropping funnel was placed in the top of the flask, purged, and capped with a rubber septum. A Hamilton gas-tight syringe was used to transfer $Fe(CO)_5$ (7.9 mL, 0.06 mol) into the funnel. The $Fe(CO)_5$ was added as slowly as possible, and the reaction flask never became more than slightly warm during addition. An additional 5 mL dry THF was used to rinse the funnel after addition was complete. After stirring overnight, the dropping funnel was removed and a fritted Schlenk tube with a catch-flask was put in its place. The reaction flask was cooled for one hour in a

dry-ice/isopropanol slush bath to form filterable crystals. The apparatus was carefully inverted to achieve filtration of the reaction mixture. Argon was used to maintain positive pressure on the reaction flask, while a vacuum was pulled on the catch-flask with a dual-stage vacuum pump. The filter-cake was kept slightly wet with THF, and then rinsed into a clean, dry, Ar-purged 100 mL Schlenk flask using a small amount of dry THF. Degassed and deionized water (30 mL) was added to the reaction flask. Great care was taken to keep the air exposure to a minimum, since the intermediate product ($Na_2Fe_2(CO)_8$•THF) is very reactive with oxygen. The dropping funnel was then reaffixed and $(C_2H_5)_4NBr$ (13.845 g, 0.0659 mol) in 30 mL degassed and deionized water was added slowly. A brick-red precipitate formed immediately and was filtered as before. The product was then washed with 60 mL degassed and deionized water, 2 x 60 mL dry THF, and 2 x 60 mL absolute ethanol. All reagents used for washing (except for water) were first cooled in a dry-ice/isopropanol slush-bath for at least 15 minutes. The product was then dried under vacuum to constant weight, giving 10.341 g (58%) of $[Fe_2(CO)_8][(C_2H_5)_4N]_2$. Due to the possibility of finely divided Fe being present in the final product, it was transferred quickly into the dry-box and stored in the freezer at -30 °C.

$Fe_2(CO)_8(\mu\text{-}CH_2)$

In the dry box, $[Fe_2(CO)_8][(C_2H_5)_4N]_2$ (4.14 g, 0.007 mol) was weighed into a 100 mL Schlenk flask. Once this was set up under a hood and connected to Ar, approximately 25 mL dry acetone was added. The flask was immersed in an ice/NaCl bath and stirred continuously for two hours. An addition funnel was placed atop the flask and 5 mL of

dry, 0 °C acetone was syringed into it. A Hamilton gas-tight syringe was used to add CH_2I_2 (0.64 mL, 0.008 mol), which was added as slowly as possible over a 20 minute period. The mixture stirred for an additional hour, and was then filtered as before, and washed with dry, 0 °C acetone until the washings appeared pale yellow. The solid was transferred to a beaker and stirred with 20 mL deionized water for about one hour. The product was then filtered through a regular fritted funnel in atmosphere, and washed with 3 x 10 mL cold (0 °C) acetone. After drying under vacuum to constant weight, the yield was calculated as 31% (0.7508 g). Infrared spectroscopy (Figure 8) and ^1H NMR (Figure 9) showed bands which were consistent with literature values. The other two peaks in the NMR spectrum are due to solvent (7.3δ) and water (1.5δ)

$Fe_2(CO)_8(\mu\text{-}CD_2)$

The same procedure was followed for this synthesis, beginning with a smaller amount of $[Fe_2(CO)_8][(C_2H_5)_4N]_2$ (2.00 g, 0.003 mol), and with the appropriate substitution of CD_2I_2. This synthesis resulted in a much higher yield of 52% (0.6154 g), probably due to a less vigorous acetone wash in the final step. An infrared spectrum (Figure 10) of this product was, predictably, indistinguishable from the protonated version. Proton NMR (Figure 11) in $CDCl_3$ showed only solvent and water peaks.

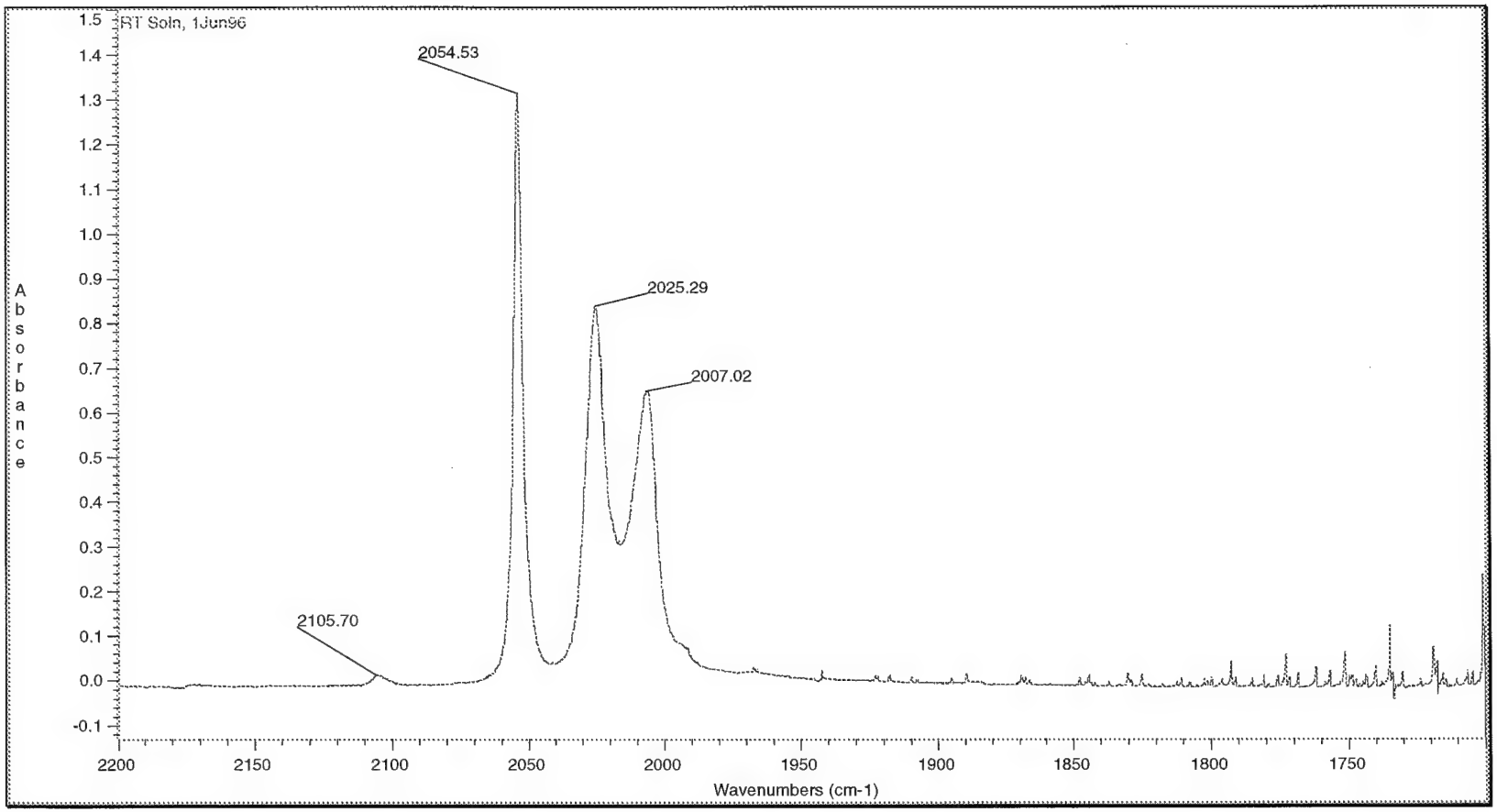

Figure 8 - - Infrared Spectrum of $Fe_2(CO)_8(\mu\text{-}CH_2)$

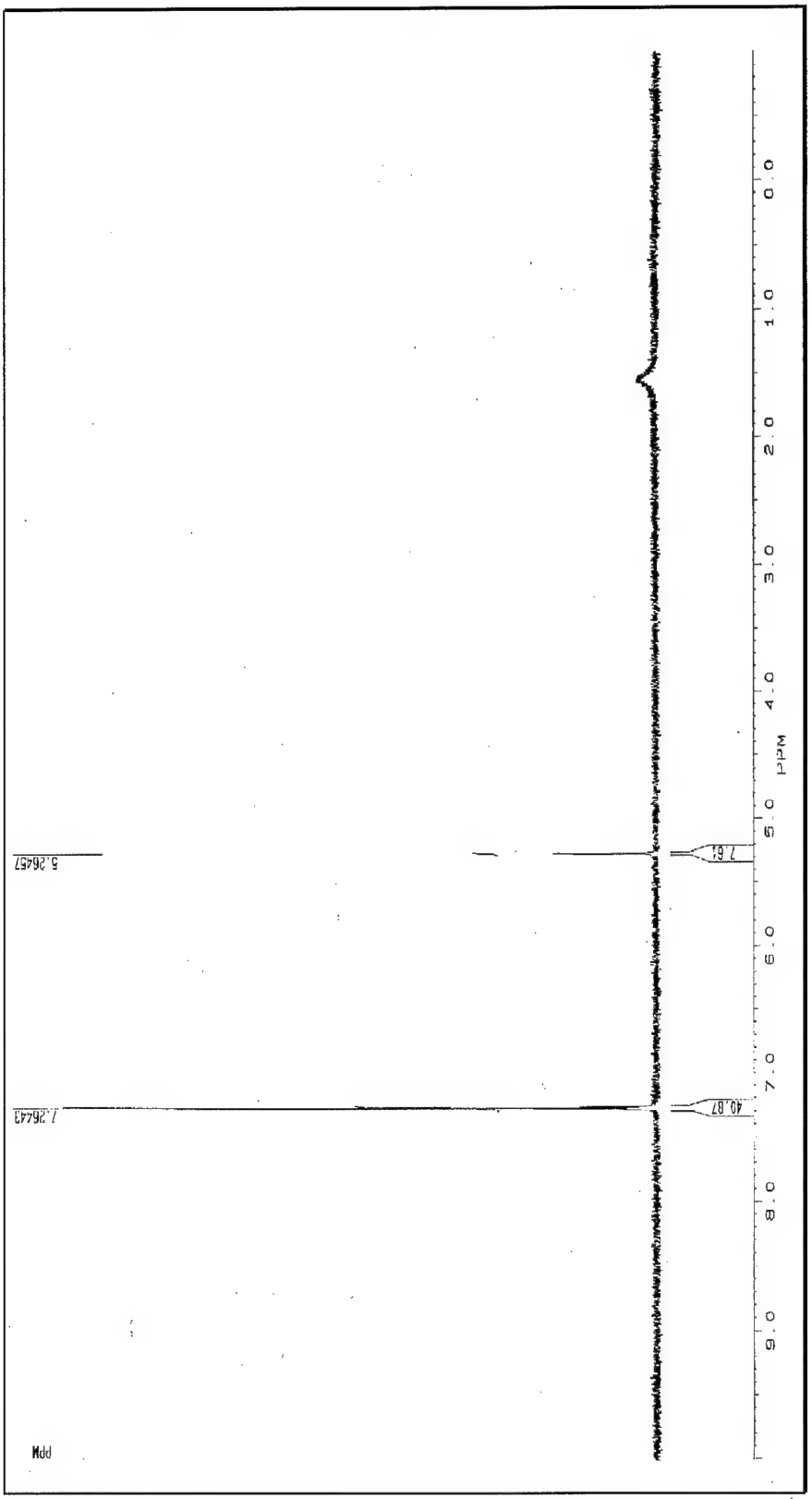

Figure 9 - Proton NMR Spectrum of $Fe_2(CO)_8(\mu\text{-}CH_2)$

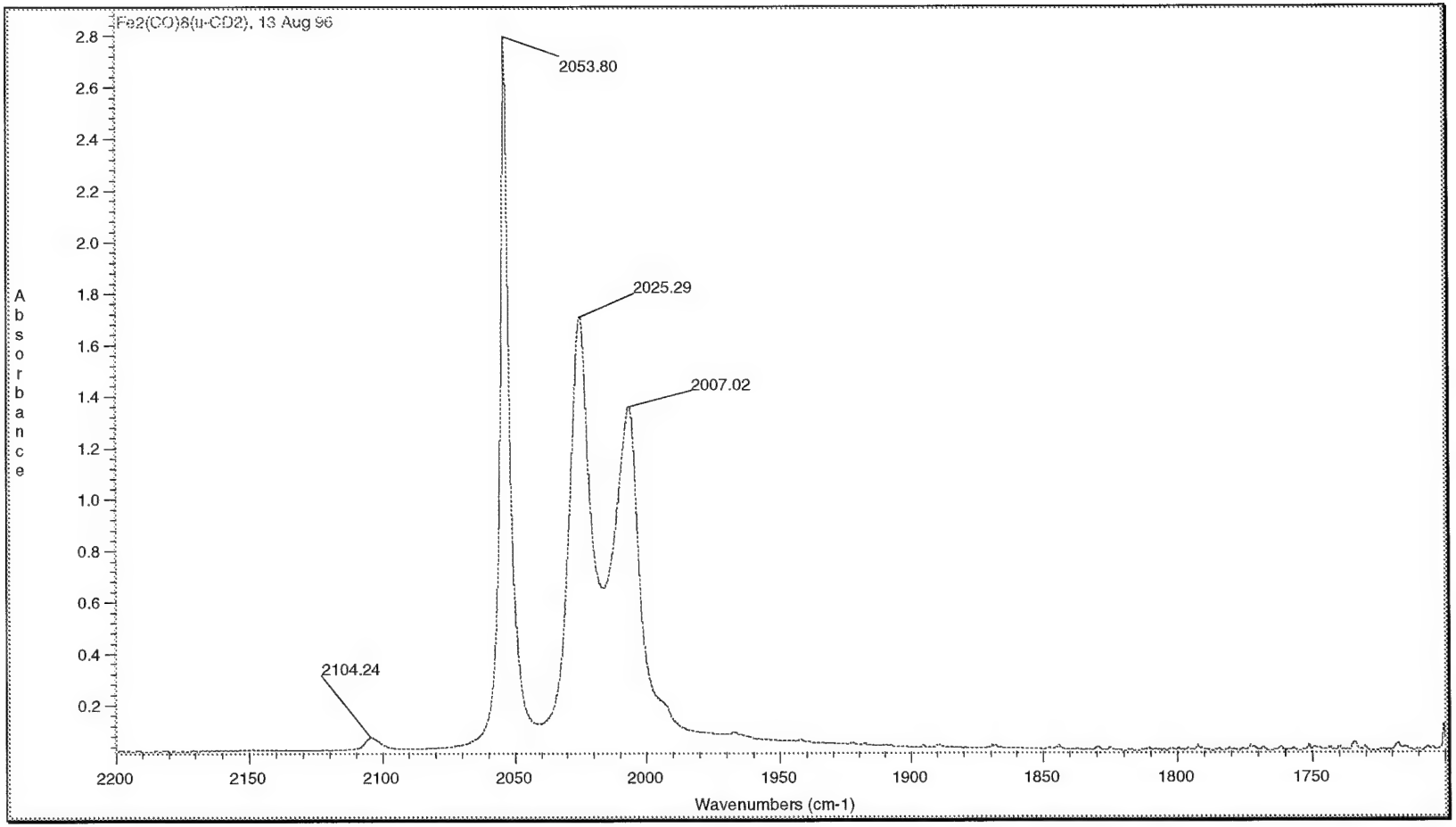

Figure 10 - Infrared Spectrum of $Fe_2(CO)_8(\mu\text{-}CD_2)$

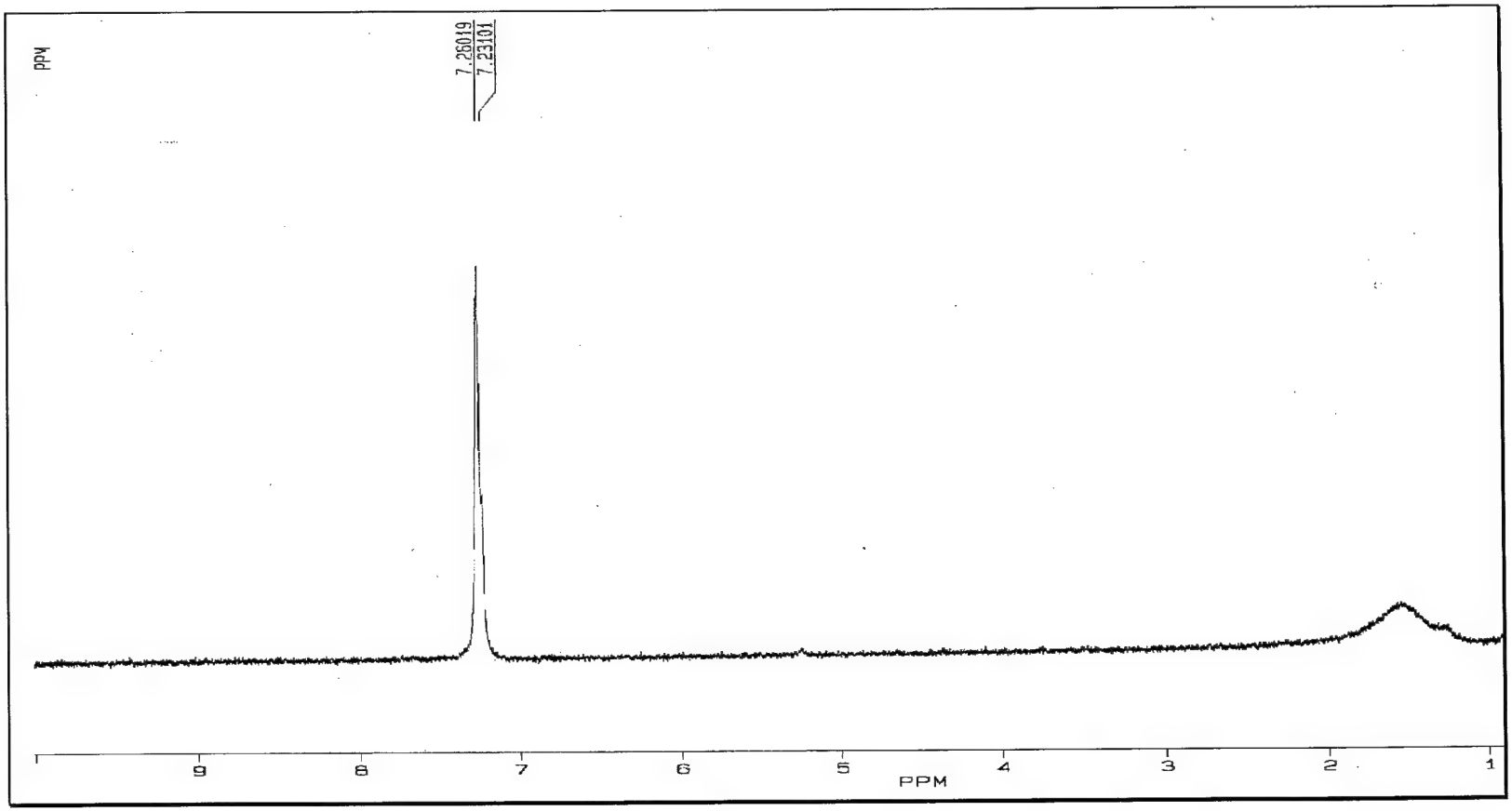

Figure 11 - Proton NMR Spectrum of $Fe_2(CO)_8(\mu\text{-}CD_2)$

Experimental Procedures

Matrix Isolation Technique

The matrix isolation studies were performed in glassing organic solvent matrices. Matrices were chosen that formed a clear, homogenous glass at temperatures of approximately 100 K. The criteria governing whether a matrix will form a glass are not well characterized. While some empirical data exists[29] there is no way to predict whether a solvent will form a glass other than to observe it upon freezing. For instance, 3-methylpentane forms a very nice glass, presumably because its branched nature precludes crystal formation. However, both methylcyclohexane and hexanes crack and become opaque upon freezing, even though they should not form crystals either. Therefore, trial and error methods were used to identify suitable mixtures of solvents. Another factor in the selection of an appropriate matrix solvent is the degree of "hardness" inherent in the system once it has frozen. This degree of hardness refers to the viscosity of the matrix after it has formed a glass[29]. Presumably, a solvent that produces a "soft" glass will allow molecules in solution to vibrate and rotate more freely. Conversely, a "hard" matrix will restrict the movement of the molecules to a higher degree. However, due to the fact that we were operating at only ~100 K, even a relatively hard organic glass could not completely isolate the solute molecules. To approach true matrix isolation more closely, one must employ techniques such as co-condensation with an ideal gas at temperatures ~10 K[30]. Table 2 lists the various solvents and mixtures that were examined in the process of choosing an appropriate matrix for our research. The bulk of

the spectra were taken in matrix 5 (from Table 2) since **1** is very photo-labile and the softer matrices such as matrix 1 allowed too many side products to form, resulting in indistinct spectra. Unless otherwise indicated, the terms "soft matrix" and "hard matrix" will refer to mixtures 1 and 5 from Table 2, respectively.

The matrix mixture was prepared in the dry-box in a clean, dry volumetric flask. For example, 0.5 mL 3-MP would be transferred to a 5 mL volumetric using a 1.0 mL Hamilton gas-tight syringe. The volumetric would then be filled to the mark with methylcyclohexane, resulting in a 90/10 mixture. Volume ratio was used in lieu of mole ratio because it was only a 10 μL difference in volume, and the volume ratio was more easily reproduced. A sample of the pure matrix would then be transferred to the cell, and a spectrum taken for use as the background. This enabled us to use solution spectra directly without explicitly subtracting the solvent spectrum. The background was collected at both room temperature and at the matrix isolation temperature (98 - 100 K). During the two hours needed to warm the cell to room temperature, a solute sample would be weighed into a 2 mL volumetric and taken into the dry box for preparation of the solution. Room temperature and low temperature spectra were taken of the solution to use as starting points. The low temperature was maintained

Matrix	Composition	Observations
1	100% 3-MP	good glass, indistinct spectra, prob. due to softness of matrix
2	100% Methyl-THF	interaction with solute at 30 °C
3	100% Methylcyclohexane	cracks and becomes opaque
4	100% Hexanes (mixture)	cracks and becomes opaque
5	10% 3-MP in Methylcyclohexane	good glass, v. sharp peaks in spectrum, assume to be "hard"
6	10% 3-MP in Hexanes	cracks and becomes opaque
7	50% 3-MP in Hexanes	cracks and becomes opaque

Table 2 - Matrix Selection

by adding liquid N_2 to the dewar as needed. The course taken after this point depended upon the nature of the experiment. Individual experiments will be fully described in Chapter 3. However, all experiments involved UV photolysis at some point. This was carried out using a 200W medium pressure Hg lamp from Oriel Corporation (66007 UNIV ARC lamp). Infra-red radiation was removed by a distilled water filter. The low-temperature cell (mounted in the dewar assembly) was placed on a specially designed variable-height platform and positioned on an optical bench at approximately 40 cm from the Hg lamp. This distance was used for all experiments for purposes of reproducibility, and to minimize sample heating due to any infra-red radiation remaining. The lamp height and height of the dewar/cell assembly remained constant, but the focus of the lamp was adjusted each time for maximum light flux through the sample. This was accomplished by adjusting the focus until the image projected behind the cell was as sharp as possible. In order to increase the photon efficiency of the impinging light, aluminum foil was placed over the rear window of the cell dewar. Photolysis periods were timed using a digital stopwatch, although all times are approximate, and only repeatable within about 5 seconds.

Data Analysis

Infrared Data. Data collected on the Nicolet Magna IR 550 was processed on a personal computer workstation using Nicolet's *Omnic 2.1* software. *Omnic* is a versatile program which allowed us to manipulate the data using a variety of methods. Normal data collection was performed using the following options:

- 32 scans per spectrum with a resolution of 0.5 - 1.0 cm^{-1}: This allowed

reasonably fast collection (~1.5 min.) with a reasonable signal-to-noise ratio. Data spacing ranged from 0.2 cm^{-1} to 0.4 cm^{-1}, depending on the resolution.

- Apodization: Either "boxcar" or "Happ-Genzel" apodization was used. Happ-Genzel was used normally, since it suppresses side-lobes more effectively and retains higher resolution than triangular apodization. In cases where maximum resolution was needed, boxcar apodization was used.

After the data were collected, the spectra usually needed some fine-tuning to baseline it properly. This was performed using the following procedure:

1. Two regions of the spectrum were reduced to a straight line using the *straight-line* function: 2400 - 2300 cm^{-1}, and 1500 - 1600 cm^{-1}. Neither of these regions were expected to contain useful data, and were nearly flat already.
2. Using the inherent function in *Omnic*, the spectrum was baselined by setting 2350 cm^{-1} and 1550 cm^{-1} to zero. This allowed for direct comparison of the spectra by overlaying them (on a computer screen) and aligning the two flat-line regions.

Many of the spectra we collected appeared to have several overlapping peaks. Deconvolution of these peaks was performed using the *Fourier Self-Deconvolution* (FSD) and *Second Derivative* (SD) functions. The SD function was used to determine the presence of "shoulders", since it would transform them into actual peaks. The FSD function was used to determine the number of peaks within broad features of the spectrum Another highly useful technique that we employed was the use of subtraction spectra. After one spectrum was subtracted from the other, one could observe which peaks had

increased in intensity and which had decreased during the time period between the spectra. However, in order to obtain the actual peak intensities of the overlapping peaks, it was neccessary to use a curve-fitting program. To this end, Jandel Scientific's *Peakfit 3.11* performed admirably. All IR curves were fit to Lorentzian line-shapes using a 99% confidence level.

UV-Visible Data. The OLIS-17 software, used to collect and store the UV-Vis data, was not particularly easy to use and had some limitations in its ability to manipulate spectra. Therefore, data was exported to a comma-delimited format and imported into another program, such as Microsoft® Excel. In this format, the data could be easily graphed, subtracted, or multiplied. Curve-fitting and peak deconvolution was performed using Jandel Scientific's *Peakfit 3.11*.

RESULTS AND DISCUSSION

"Whoever, in the pursuit of science, seeks after immediate practical utility, may generally rest assured that he will seek in vain."

Hermann von Helmholtz

Overview

The photochemistry of **1** and **2** was studied in both hard and soft matrices, yielding distinctly different results. The soft matrix (neat 3-methylpentane) allowed the molecule to assume the energetically favorable D_{3h} conformation upon reaching ~98 K (Figure 12). During photolysis in this matrix (Figure 13), the resulting bands were indistinct and poorly resolved. Conversely, the hard matrix (10% 3-methylpentane in methylcyclohexane) resulted in sharp, well-defined peaks. This was true for both the starting material (Figure 14), which retained C_{2v} symmetry upon freezing, and the spectra taken during photolysis (Figure 15). In either matrix, however, both **1** and **2** proved extremely photolabile, forming CO-loss products after less than one minute of photolysis. This was not entirely unexpected, since $Fe_2(CO)_9$ is *extremely* photo-active[2e], and the μ-CH_2 would be expected to compete for electron density with *trans* carbonyls to a much higher degree than μ-CO.

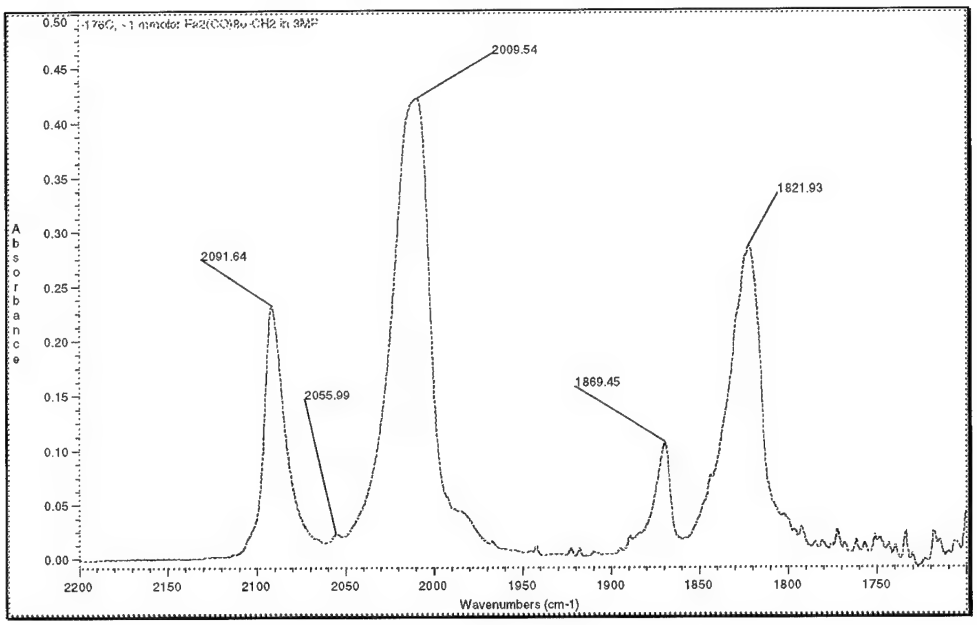

Figure 12 - Infrared Spectrum of $Fe_2(CO)_8(\mu\text{-}CH_2)$ in the Soft Matrix at 97 K

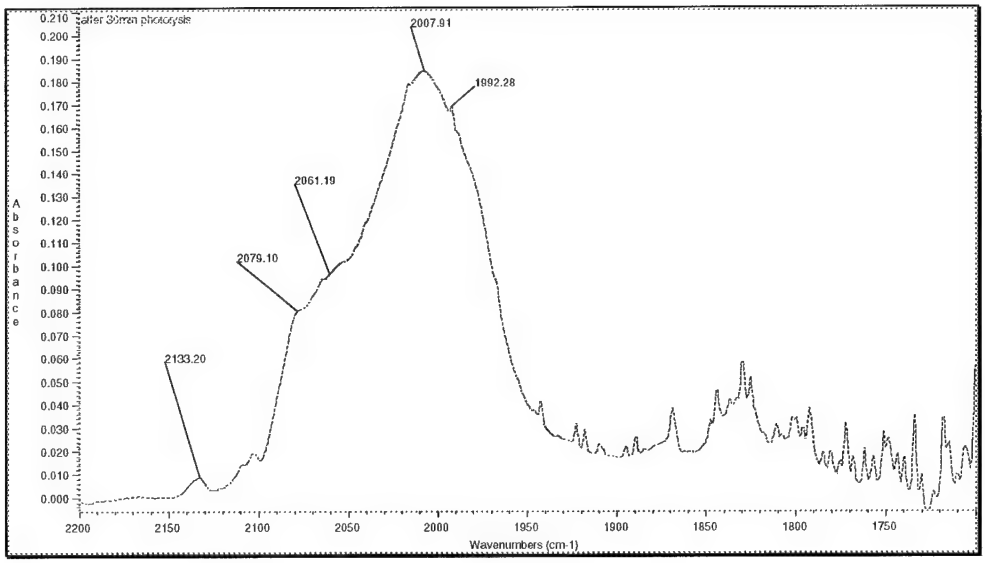

Figure 13 - Infrared Spectrum of $Fe_2(CO)_8(\mu\text{-}CH_2)$ after 30 Minutes of Photolysis(97 K) in the Soft Matrix

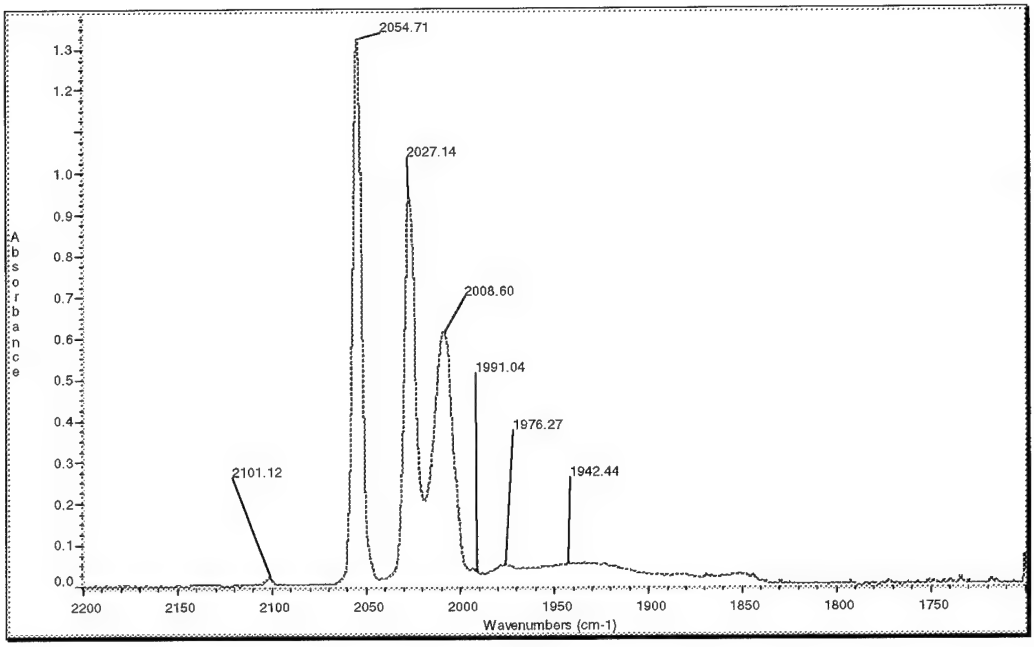

Figure 14 - Infrared Spectrum of $Fe_2(CO)_8(\mu\text{-}CH_2)$ in the Hard Matrix at 98 K

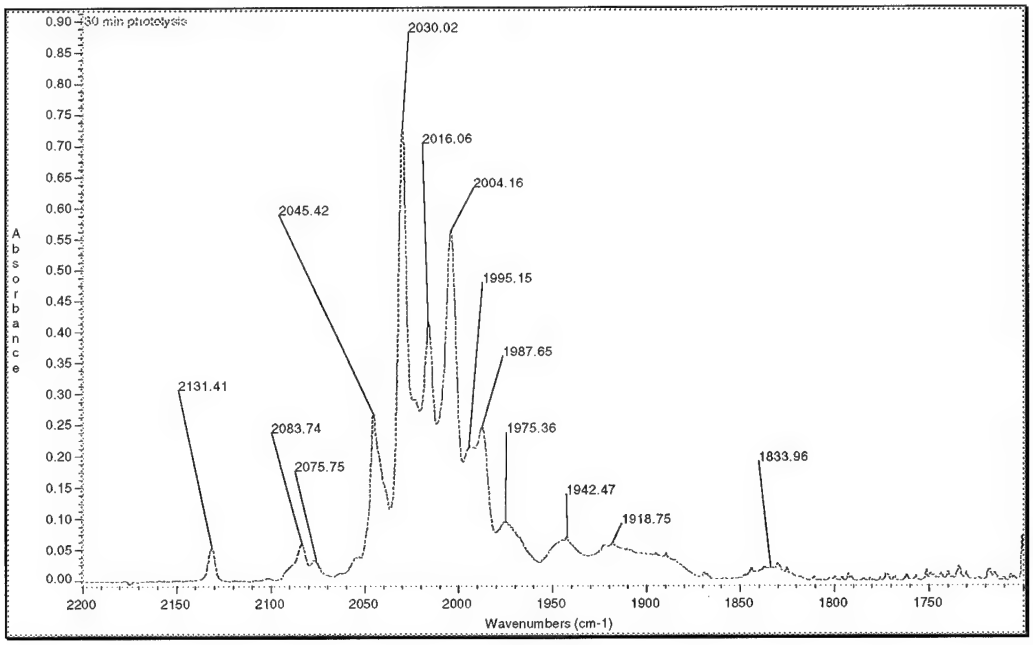

Figure 15 - Infrared Spectrum of $Fe_2(CO)_8(\mu\text{-}CH_2)$, after 30 Minutes of Photolysis(98 K) in the Hard Matrix

Photolysis of $Fe_2(CO)_8(\mu\text{-}CH_2)$ in a Hard Matrix

First CO-Loss Product

After only 40 seconds of photolysis, **1** is observed to liberate free CO (~2032 cm^{-1}) and form a CO-loss product. Figure 16 shows a difference spectrum between 40 seconds of photolysis and the starting material. Already evident are the main features of what seems to be a single CO-loss product. The starting material is clearly consumed, with its main bands appearing as negative peaks after subtraction. The new species shows infrared peaks at the following locations: 2093, 2085, 2030 and 1987 cm^{-1}, with possible peaks at 2021 and 2003 cm^{-1}, and a broad feature centered at 1920 cm^{-1}. As the photolysis period is lengthened, these peaks are seen to increase, and a new peak appears at 2045 cm^{-1}, after about 5 minutes (Figure 17). After 10 minutes, the peaks assigned to product #1 (**3**) decrease steadily. Figure 18 shows the difference between 180 minutes and 5 minutes, emphasizing the disappearing peaks due to **3**. Note that CO continues to be produced over this period, and that the negative peaks due to remaining **1** are labeled "parent". If **3** is a CO-loss product at all, is it the result of single or double CO elimination? If it were a single CO-loss product, one might reasonably expect to see bridging carbonyls, since the molecule would be an unbalanced, 18/16-electron complex. However, **3** exhibits no bridging or semi-bridging carbonyls, which should appear between 1700 and 1900 cm^{-1}. It is obvious we need a method of quantitating both the loss of **1**, and the formation of free-CO and **3**. The obvious choice in this instance is the use of molar absorptivity (ε).

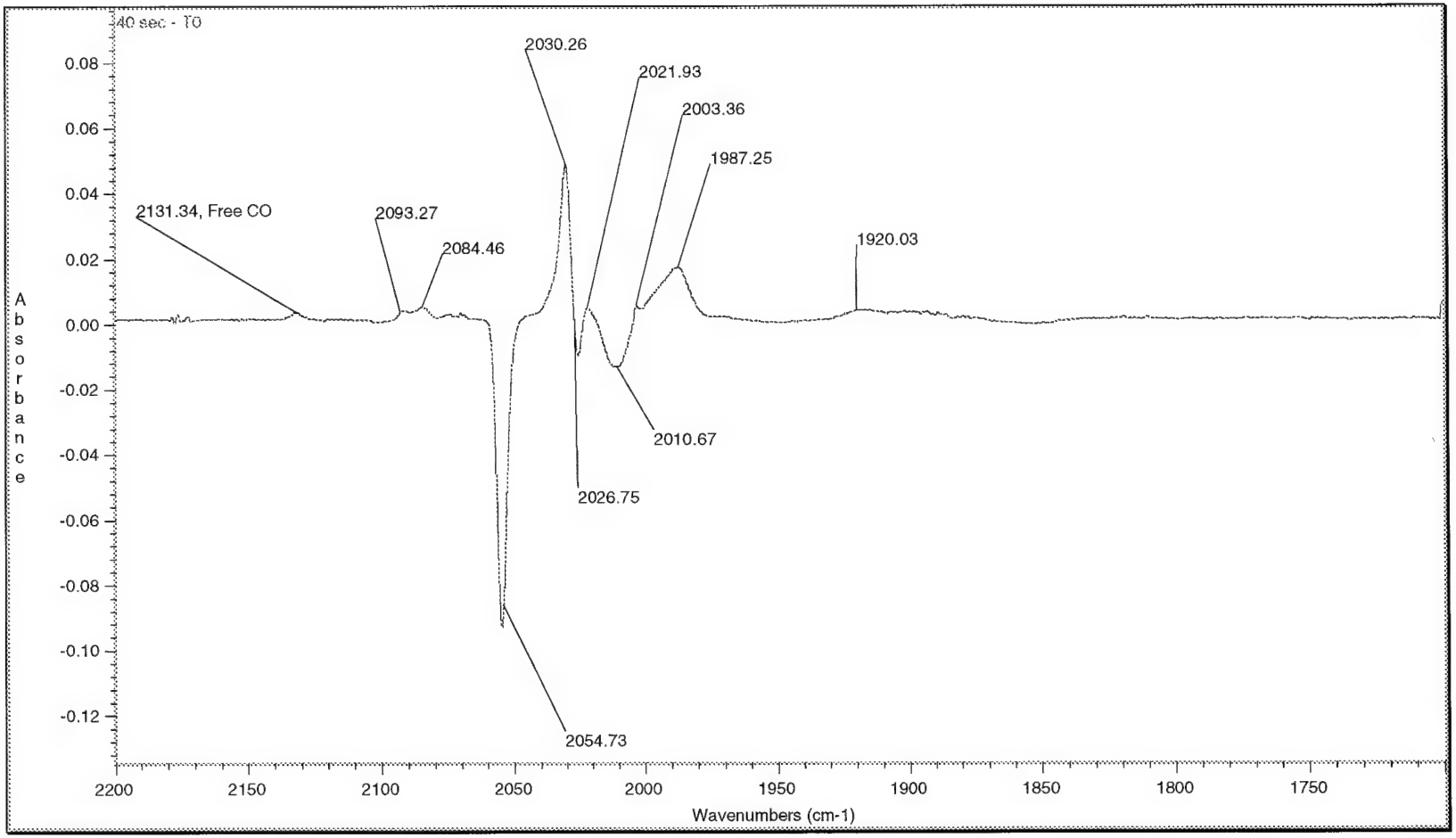

Figure 16 - Difference Infrared Spectrum between 40 Seconds and 0 Seconds Irradiation

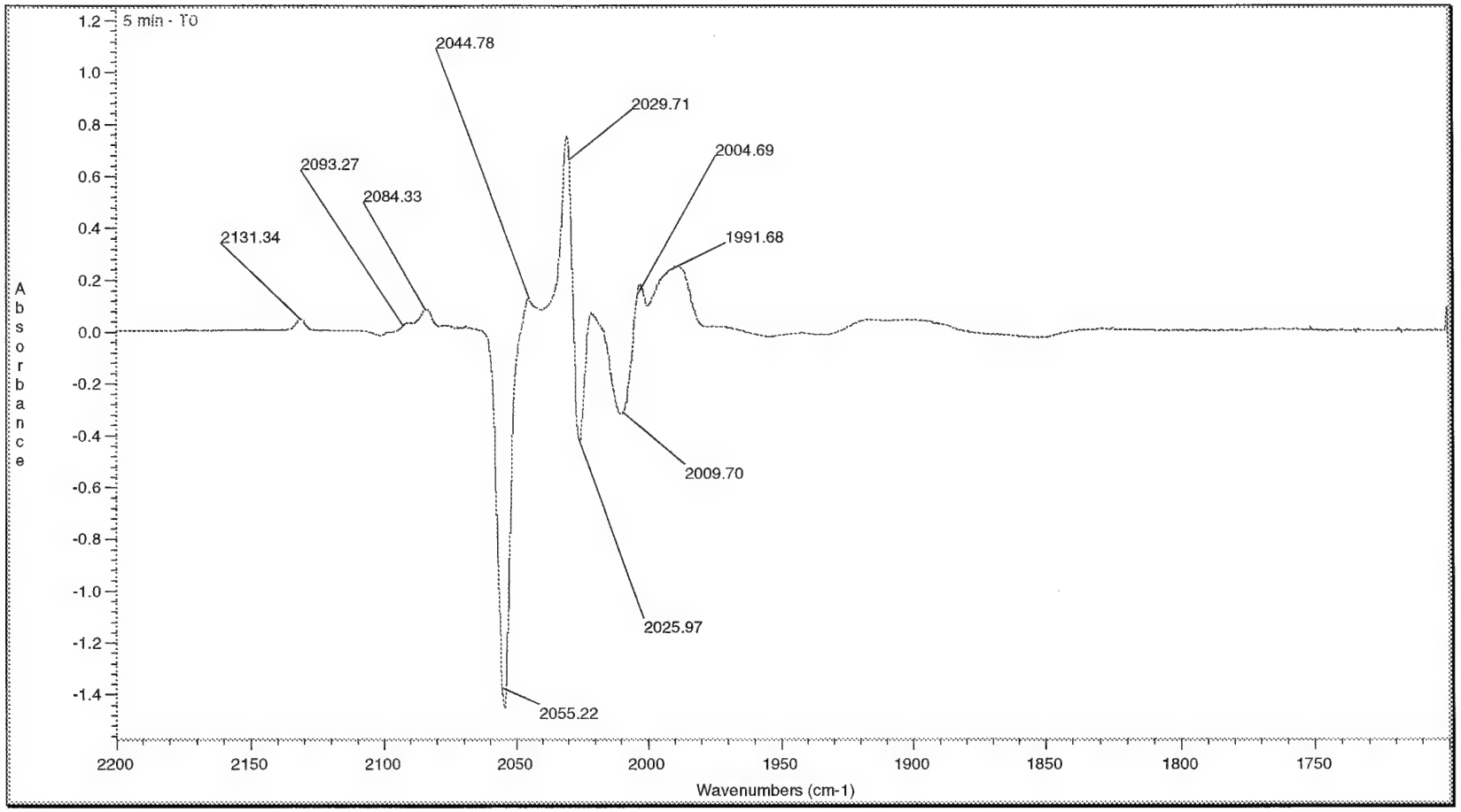

Figure 17 - Difference Infrared Spectrum between 5 min and 0 Minutes of Iirradiation

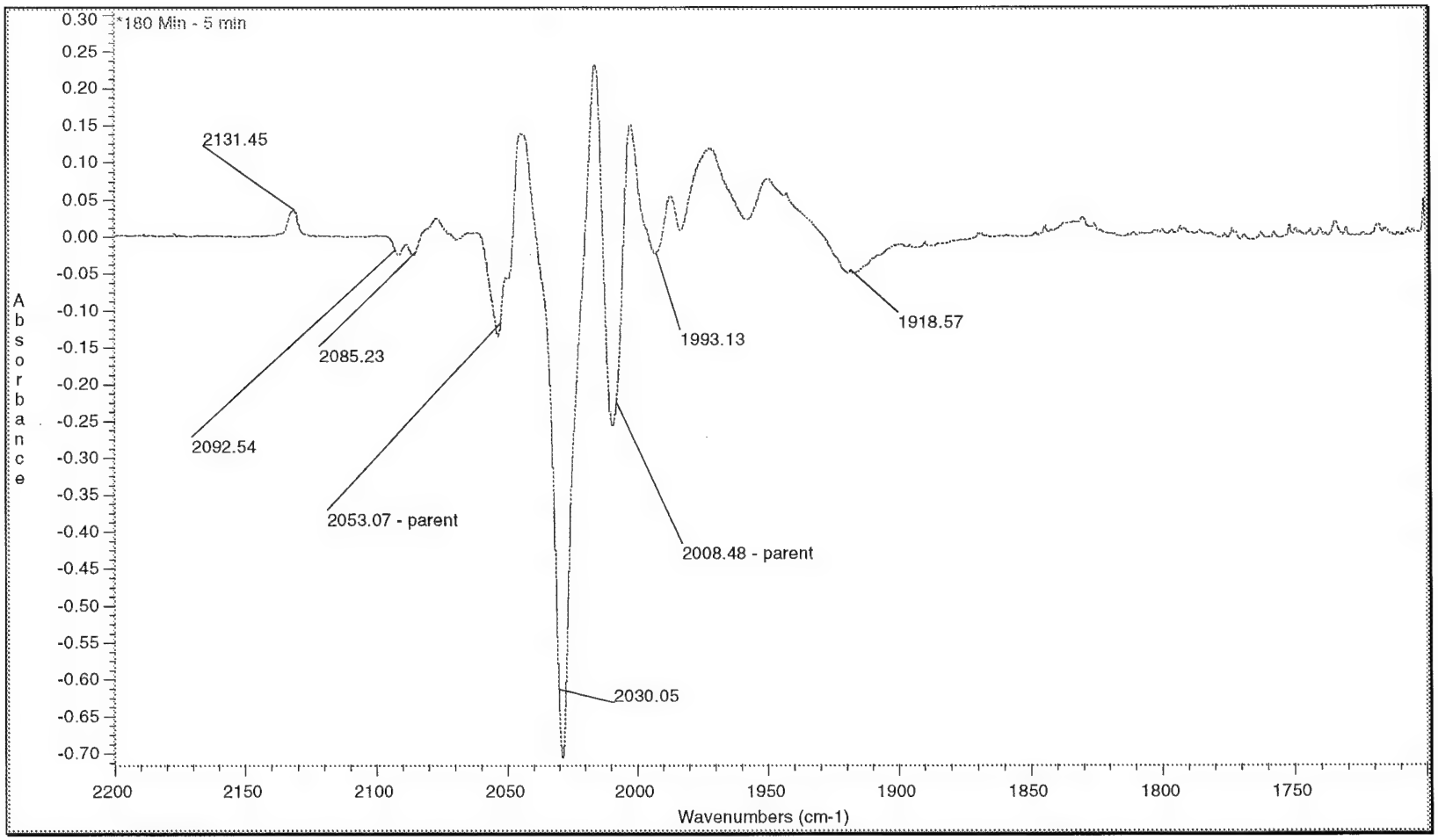

Figure 18 - Difference Infrared Spectrum between 180 min and 5 Minutes of Iirradiation, Emphasizing Negative Peaks

This was elementary for CO and **1**, and only slightly more difficult for **3**. As measured by Pope and Wrighton[31], carbon monoxide in an alkane matrix has a value of ε equal to 400 M^{-1} cm^{-1}. To determine the value of ε for **1**, a Beer's Law plot was created from the infrared spectra of a series of dilutions, and the slope of the least-squares line was calculated (Table 3 and Figure 19). This analysis was only performed for the three major peaks at 2055, 2025, and 2006 cm^{-1}. Even though these peaks shifted somewhat at <100 K, the values of ε were considered valid at low temperatures for our purposes.

To calculate a value for **3**, we made use of the observation that it was virtually the only product being formed within the first 5 minutes of photolysis. Using infrared data from each minute of the first five, a 1:1 molar ratio of Δ**1** to Δ**3** was assumed, and the concentration of **3** was calculated for each minute. This data was used to create a Beer's Law plot for the major peak of 2030 cm^{-1} (Table 4 and Figure 20).

Methylene Bridged (from 3 Oct 1996)															
b*c	A(2055)					A(2025)					A(2006)				
3.02E-04			*Regression Statistics*			2.896413	*Regression Statistics*				2.462071		*Regression Statistics*		
2.01E-04			Multiple R	0.988144		2.085726	Multiple R	0.994875			1.700499		Multiple R	0.997021	
1.01E-04	1.621657		R Square	0.976429		1.060107	R Square	0.989777			0.855625		R Square	0.994051	
5.00E-05	0.885395		Adjusted R Square	0.476429		0.601839	Adjusted R Square	0.739777			0.490079		Adjusted R Square	0.744051	
2.50E-05	0.509889		Standard Error	0.08683		0.364197	Standard Error	0.107657			0.309475		Standard Error	0.069548	
			Observations	3			Observations	5					Observations	5	
epsilon:	16569.44					9937.249					8307.434				

Table 3 - Least-squares Fit Data for ***1***

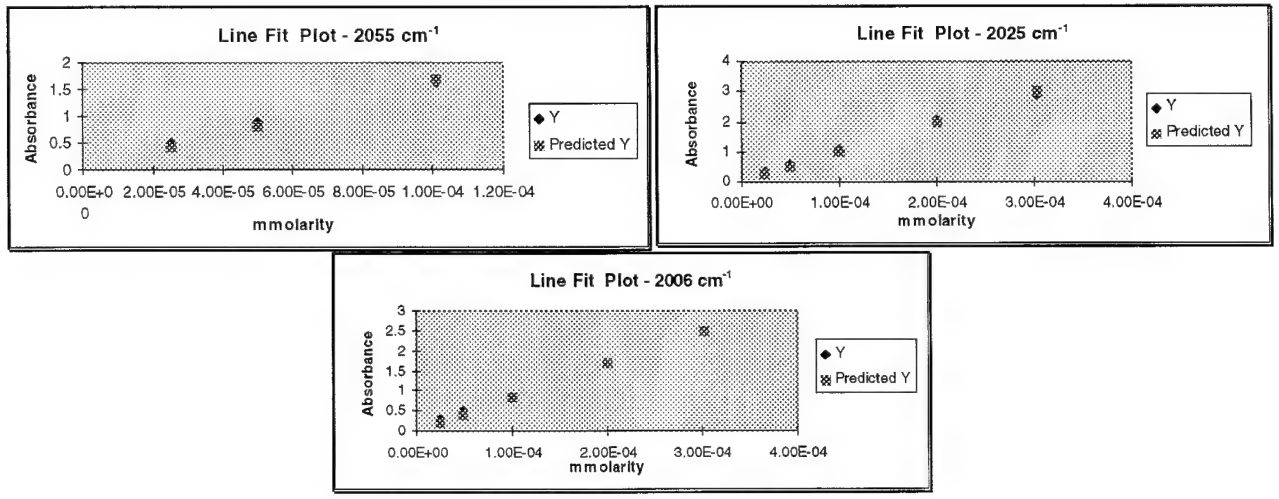

Figure 19 - Linear Regression Graphs for the Three Major Peaks of $Fe_2(CO)_8(\mu\text{-}CH_2)$

First Photo-Product (from 1 June 1996)					
Min. Irrad.	b*c	A(2030)		*Regression Statistics*	
2	6.16E-05	0.51778		Multiple R	0.996025
3	7.86E-05	0.683915		R Square	0.992067
4	8.62E-05	0.731281		Adjusted R Square	0.658733
5	8.9E-05	0.755743		Standard Error	0.009545
				Observations	4
	epsilon:	8524.17			

*Table 4 - Least-squares Fit Data for **3***

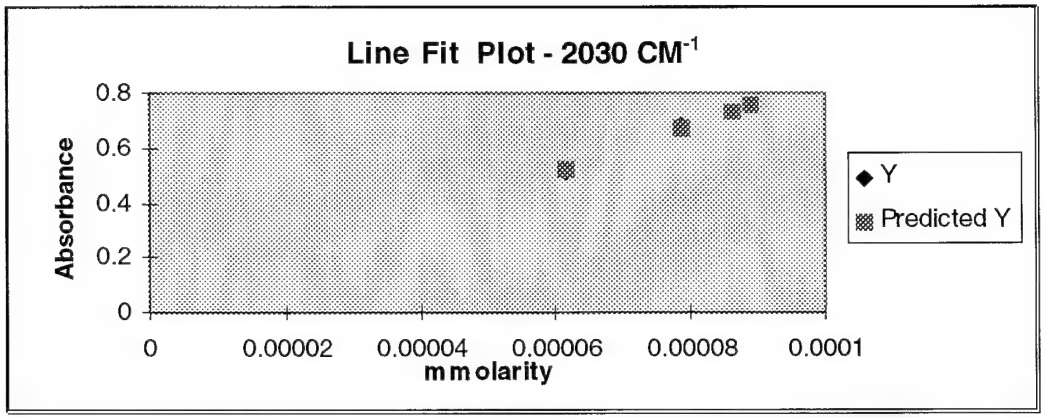

*Figure 20 - Linear Regression Graph for **3***

After calculating these values, we used them to determine whether **3** was indeed a single CO-loss product, or the result of double CO-loss. To determine this, we calculated molar ratios of $\Delta CO/\Delta \mathbf{1}$, $\Delta CO/\Delta \mathbf{3}$, and $\Delta \mathbf{1}/\Delta \mathbf{3}$, where $\Delta\xi$ indicates the change in the concentration of ξ in units of millimolarity. A ratio of approximately unity for each of these would indicate the following, respectively:

- There is only one CO being lost per molecule of **1**.
- There is only one molecule of **3** being formed for each molecule of CO.
- Compound **3** is the only product being formed at that given point in time, and is therefore the single CO-loss product of **1**.

The results of these calculations are listed in Table 5, and support the above conclusions.

Molar Ratios of CO, *1* and *3*			
Date of Experiment	$\Delta CO/\Delta \mathbf{1}$	$\Delta CO/\Delta \mathbf{3}$	$\Delta \mathbf{1}/\Delta \mathbf{3}$
11 Apr, 5 min. irradiation	0.96	0.98	1.02
1 June, 1 min. irradiation	0.98	0.92	0.94
1 June, 2 min. irradiation	1.06	1.03	0.97
1 June, 3 min. irradiation	1.13	1.08	0.95
1 June, 4 min. irradiation	1.11	1.12	1.01
1 June, 5 min. irradiation	1.2	1.19	0.99
14 July, 5 min. irradiation	1.13	1.19	1.06
13 August, 5 min. irradiation	1.05	1.15	1.1
Averages:	1.08	1.08	1.01

Table 5 - Molar Ratios (Absolute Values) of CO, 1 and 3

The formation of an asymmetric, single CO-loss product is unusual, due to the propensity to adhere to the "18-electron rule". The lack of a bridging carbonyl ligand is especially surprising in this case, because the small size of the iron atoms should offer little

resistance to bridging. Undoubtedly, the hardness of the matrix is at least partly responsible for this phenomenon. However, it seems unreasonable that the rigidity of the matrix alone could prevent a carbonyl ligand from assuming a bridging geometry. It is likely that the excellent π-accepting ability of the μ-CH_2 ligand acts to stabilize the molecule in some fashion. It may act as a conduit for electron density so that the electron imbalance, if it exists, may be partly ameliorated. If we assume that the molecule has remained intact, there is another structural option which, though unlikely, would allow each iron to attain an 18-electron configuration. This would require that the methylene bridge convert to a carbene group on the CO-donating iron, and that an iron-iron double bond be formed. These potential structures are illustrated in Figure 21.

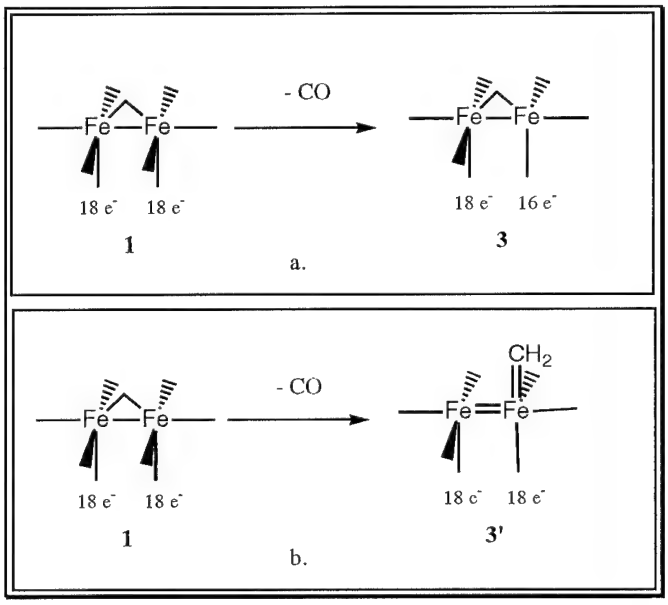

Figure 21 - Possible Structures for ***3***

Second CO-loss Product

After further irradiation, a second set of peaks begins to appear. This new product, or products, begins to appear substantially between 5 and 10 minutes of irradiation, and continues to be produced for the remainder of the experiment. The major peaks are located at 2076, 2045, 2016, 2004, 1988, 1971, 1949 and 1833 cm^{-1} (Figure 22). It is also evident that free CO is still being produced, although at a much

slower rate. In fact, the entire system begins to slow down, almost coming to a complete halt after 90 minutes of irradiation. For example, the amount of free CO produced during the hour between 120 and 180 minutes is roughly 5-times less than that produced during the first *5 minutes* (Figure 23). The obvious question is, what is the structure of this new product and how many carbonyls are being lost to form it? Applying the same method we used before, we were able to determine that a double CO-loss product (**4**) is being created, and that it is being formed by the elimination of a carbonyl group from **3**. This conclusion is arrived at by examining two pieces of information: total amount of CO produced, and the molar ratio of CO production to the consumption of **3**.

Since **3** seems to reach its peak concentration after about 5 minutes of irradiation, we can use the times of 5 minutes and >90 minutes to approximate the times when **3** and **4** are respectively at maximum concentration. Comparing the free CO produced during these time periods, we observe the following facts:

- The CO produced during the first 5 and the remaining 85 to 175 minutes is approximately equal.
- The concentration of free CO after 90 to 180 minutes of photolysis is approximately twice the original concentration of **1**

	CO Produced (mmolar)				
Date of Experiment	First 5 min.	Last 85 to 185 min	Total	Initial Conc. of *1*	Ratio
11-Apr	0.525	0.725	1.25	0.67	1.87
14-Jul	0.875	0.875	1.75	0.83	2.11
13-Aug	1.925	1.6	3.525	2.04	1.73

*Table 6 - Ratio of Total CO Produced to Initial Concentration of **1**, Showing Evidence for the Generation of a Double CO-loss Product*

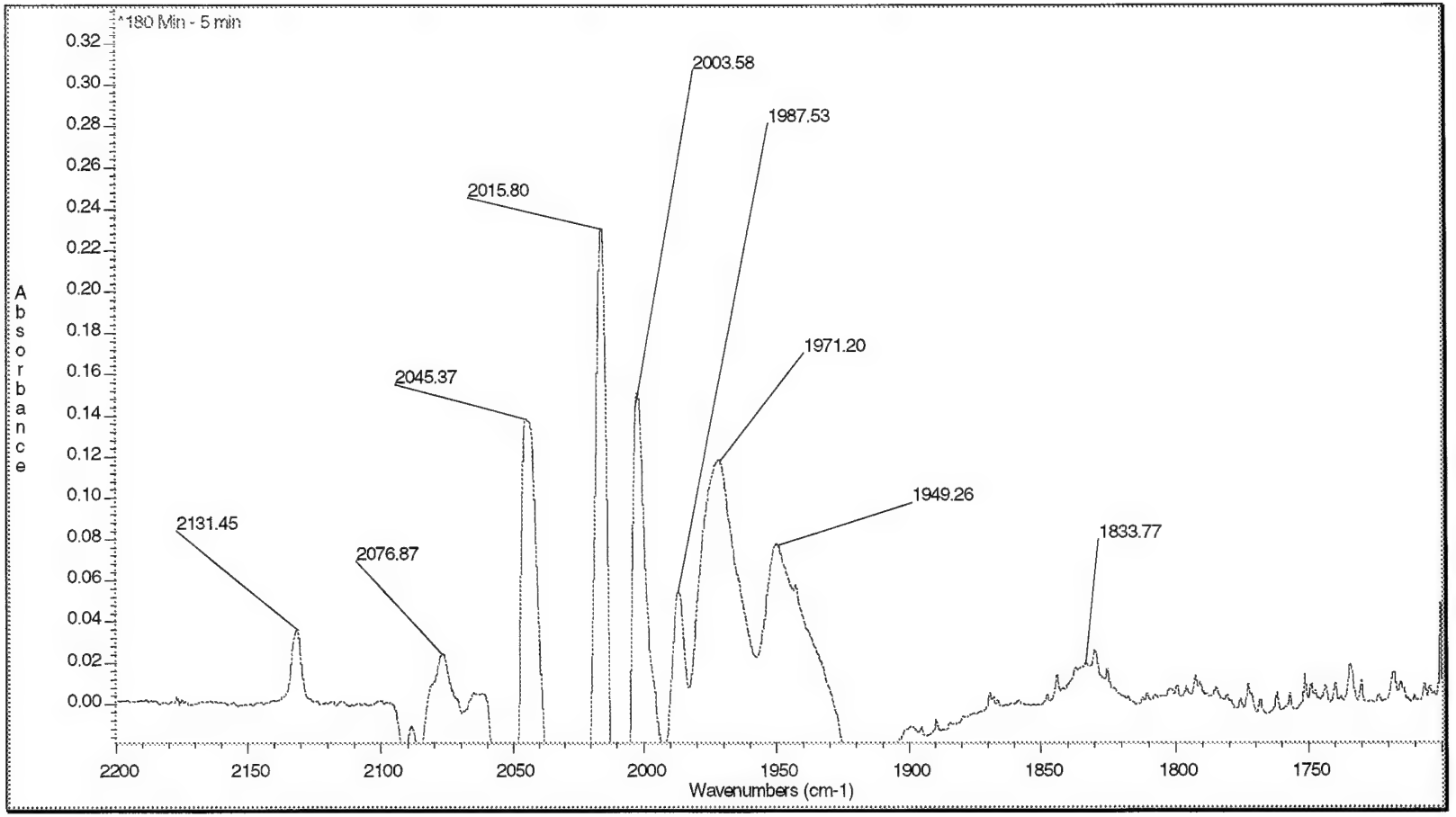

Figure 22 - Difference Infrared Spectrum between 180 min and 5 Minutes of Irradiation, Emphasizing Positive Peaks

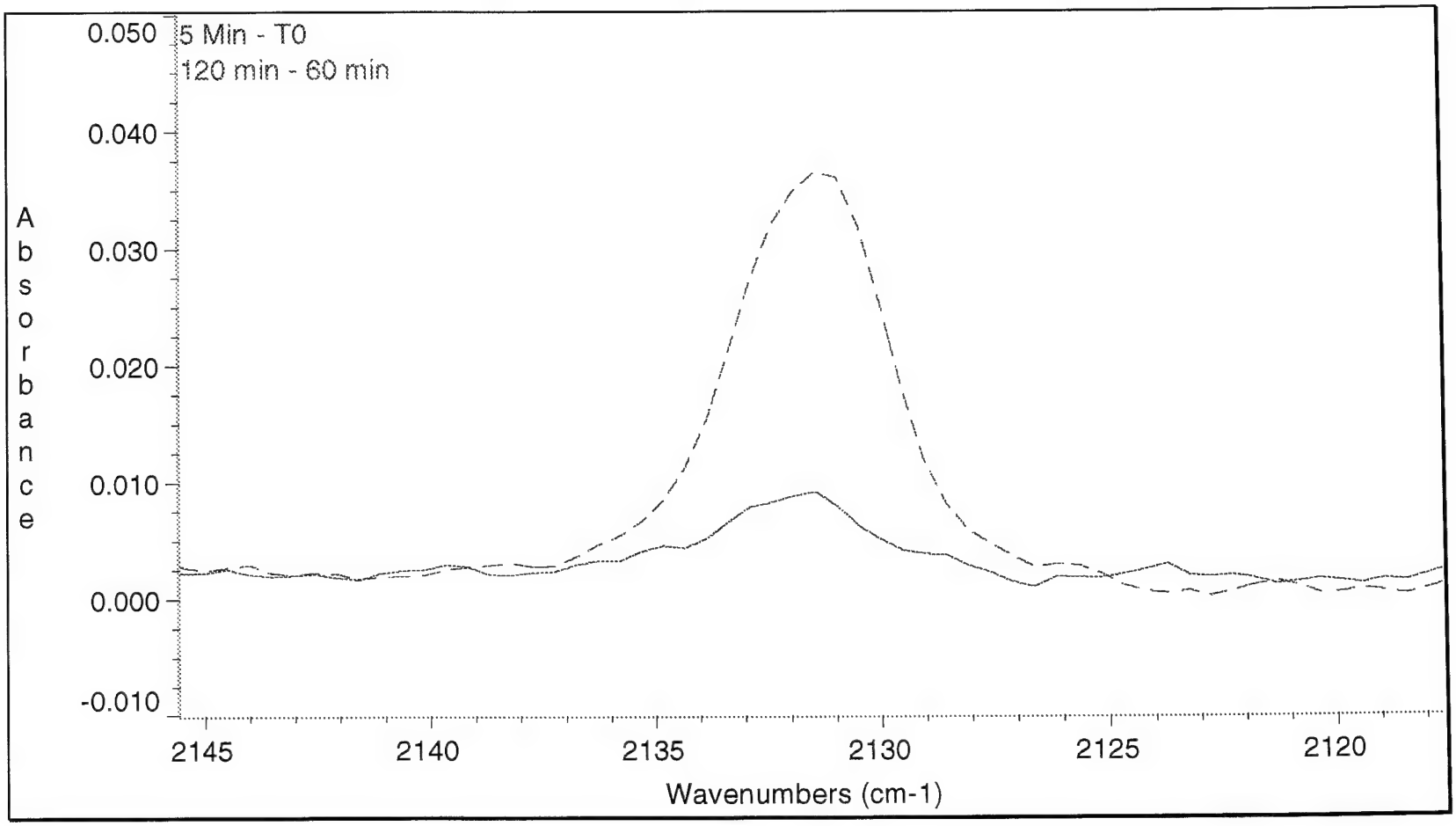

Figure 23 - Comparison of CO Production, First 5 Minutes (dashed line) vs. Last 60 Minutes (solid line)

The supporting data for these observations is summarized above in Table 6, and leads to the following conclusions:

- There *is* a double CO-loss product being formed.
- Since **1** is essentially depleted in the first 10 minutes, the second equivalent of CO must be provided by **3**.

Further evidence for the second conclusion may be obtained by comparing the depletion of **3** with the production of CO. Plotting the separate data points and their ratio for identical periods of time, we can see that, with the exception of the first fifteen minutes, they track very closely. Therefore, we may reasonably conclude that **4** is the single CO-loss product of **3**. Before discussing possible structures for **4**, based upon the above data, we should answer a critical question: "What happens to the methylene bridge?"

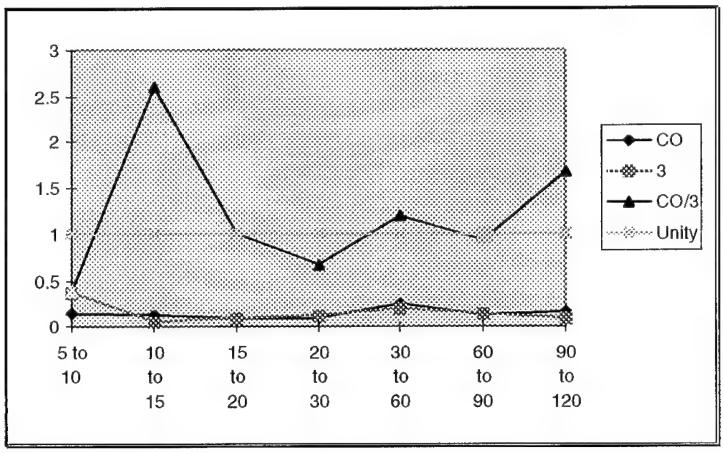

Figure 24 - Ratio of Production of CO to Depletion of 3

The Fate of the Methylene Bridge

Of course, one of the possible photochemical pathways which a molecule such as **1** might follow is metal-metal bond homolysis. Are the peaks that we observe upon the formation of single and double CO-loss products the result of several mono-metallic

compounds? To answer this intriguing question, we examined the deuterated version of the parent molecule (**2**) under similar conditions. After positively identifying the carbon-dueterium (C-D) stretching bands (Figure 25, see Table 1 for reference), we were able to monitor them throughout the entire photolysis process. After 90 minutes of irradiation, the lower-lying peak had been absorbed into the free CO peak, and the higher peak exhibited a considerable amount of shift and/or attenuation. If the peak value at 2232 cm^{-1} is measured directly after 90 minutes of irradiation, there seems to be a 30% decrease in its intensity. If the peak is measured at its shifted location of 2225, there is only an 11% decrease in intensity. Postulating that the C-D stretches should remain in the same location if the bridging ligand stays intact, it is apparent that most of the molecules retain their methylene bridge, and are therefore dimetallic. Examining data from the two experiments for which we were able to collect post-photolysis spectra, we found that a 90 minute period results in ~12% decrease in the concentration of **1**, while a 180 minute period results in ~26% decrease. This is in agreement with the data collected from **2**, and there seems to be evidence that, even in a very rigid matrix at <100 K, **1** is able to split apart and form a stable mono-metallic compound. To help us understand what was happening in the matrix, we decided to observe the behavior of 1 while it underwent room-temperature photolysis. Under these conditions, homolysis should certainly be observed, and indeed it was. What we discovered was the formation of a major product (Figure 26) with peaks which correspond to the literature values for $Fe(CO)_5$.[32] The identity of the minor product is unknown at this time. Upon examination of the matrix

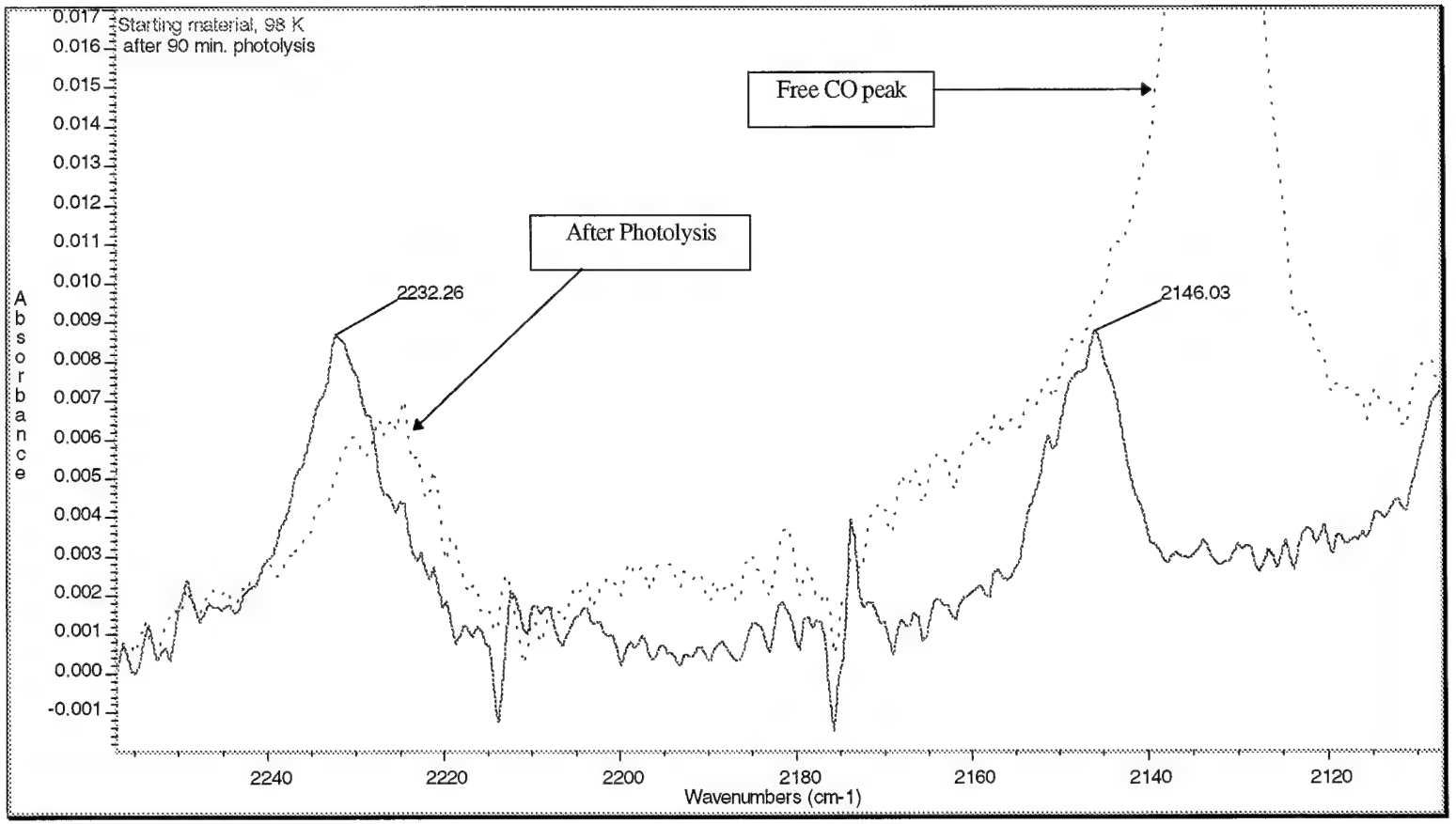

Figure 25 - Infrared Spectrum of Carbon-Deuterium Stretching Bands, Before and After Photolysis

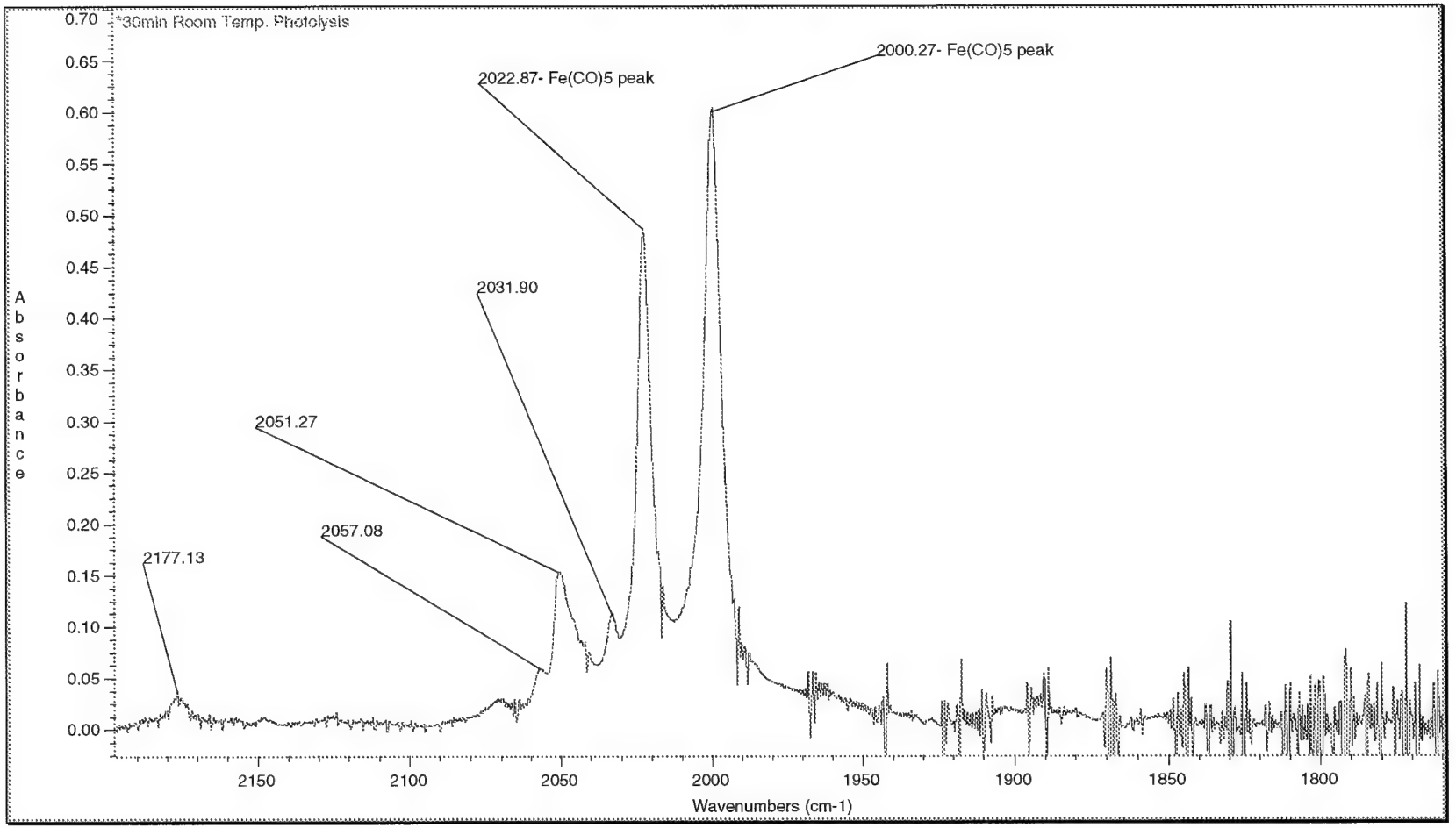

Figure 26 - Infrared Spectrum of Room Temperature Photolysis of ***1***

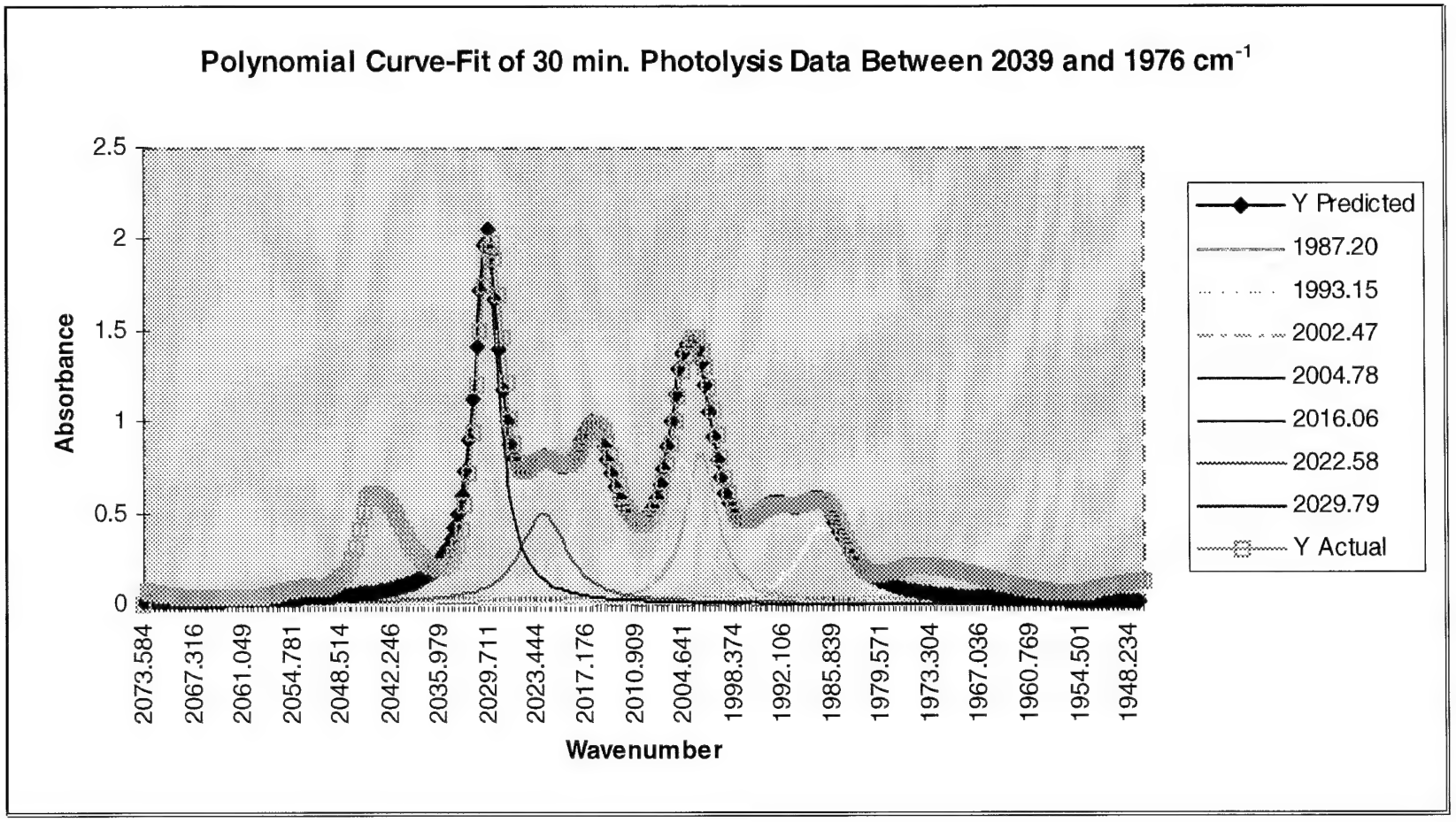

Figure 27 - Polynomial Curve-fit of Infrared Data after 30 Minutes of Photolysis in the Hard Matrix

isolation spectra, it is not readily apparent that $Fe(CO)_5$ is present. Because of the large absorbances at 2030 and 2004, the subtraction spectra do not reveal any useful information. However, performing a polynomial curve-fit yields peaks at 2023 and 2002 (Figure 27), in approximately the same ratio (1:1.2) as the peaks in Figure 26. It is our belief that these are the matrix-shifted peaks of $Fe(CO)_5$.

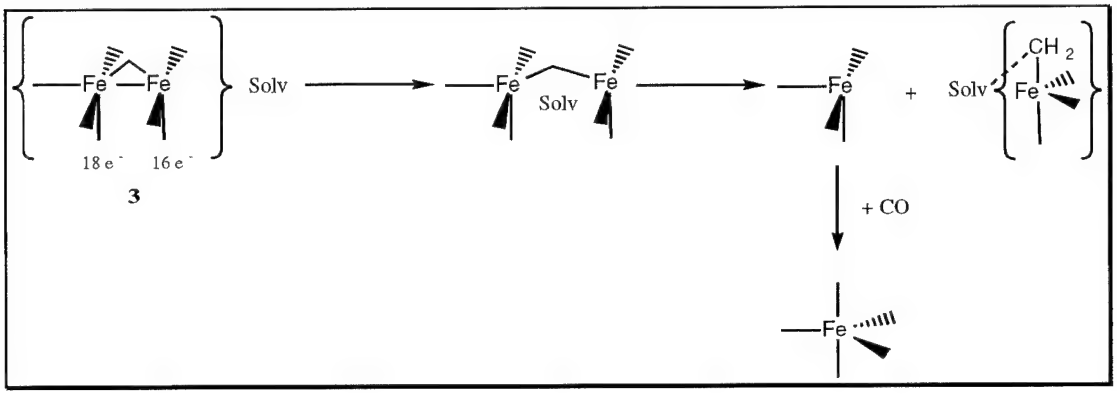

Figure 28 - Possible mechanism for inter-matrix formation of $Fe(CO)_5$

The formation of $Fe(CO)_5$ within the matrix was unexpected and quite unusual. Given that this particular matrix seems to be rigid enough to keep carbonyl ligands from bridging, it is untenable to think that two halves of either **1** or **3** could diffuse far enough away from each other to independently recombine with carbon monoxide. Therefore, there must be some feature of **3**'s structure which aids in this process. One possible solution may be found in Zhang, Zhang and Brown's study of $Mn_2(CO)_{10}$.[33] The authors investigated the photochemistry of $Mn_2(CO)_{10}$ in a frozen 3-methylpentane matrix, and discovered the existence of a *solvento* complex which subsequently converted to

$Mn_2(CO)_8(\mu\text{–}\eta^1\text{:}\eta^2\text{–CO})$. This *solvento* complex formed *immediately* upon the release of CO from the parent molecule, and had a lifetime of about ten minutes. The formation of such a complex in the case of **3** would explain the unusual stability of the unbalanced species, *and* provide a possible mechanism for the formation of $Fe(CO)_5$. In order for **3** to split apart without diffusing into the matrix, it seems necessary for a solvent molecule to act as a wedge and drive the two halves of the molecule apart. If a molecule of solvent were already complexed with **3**, it would be that much easier to engage in such a mechanism. This mechanism is depicted schematically in Figure 28.

Possible Structures Revisited

Given what we know about **3**, **4**, and the methylene bridge, we must only consider structures that contain a $\mu\text{-}CH_2$ group, and at least one μ-CO in the case of **4**. For photo-product **3**, this effectively limits us to the structure depicted in Figure 21(a), with the addition of a solvent molecule complexed with it in some fashion. For the formation of photo-product **4**, there are two possible choices, which are depicted in Figure 29.

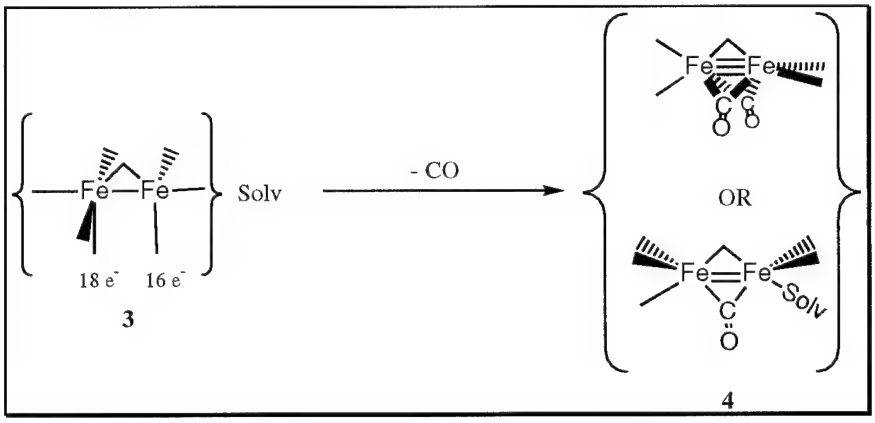

Figure 29 - Possible Structures for 4

Since there is only one bridging carbonyl peak, the doubly-bridged/doubly-bonded structure seems to be the most likely. However, given the weakness of the peak at 1833 cm^{-1}, it is possible that a second bridging peak exists and is too weak to detect.

Photolysis of $Fe_2(CO)_8(\mu\text{-}CH_2)$ in a Soft Matrix

Due to the previously mentioned problems with the 100% 3-methylpentane matrix (see Figure 13), we were able to draw very few conclusions from these data. What we did observe was that **1** seems to follow a reaction pathway similar to that followed in room temperature photolysis. That is to say, the peaks that are present after the solution returns to room temperature are very similar to those we observed after photolysis conducted at room temperature, but in different proportions (Figure 30).

Back-Reaction of $Fe_2(CO)_6(\mu\text{-}CH_2)$ with Carbon Monoxide

Upon cold, dark back-reaction of **4** with CO, we see what we would expect to see: the consumption of **4**, re-production of **3**, and possibly a very small amount of **1** (Figure 31). However, upon warming in the absence of light to ~140 K, the back-reaction proceeds through to the starting material, **1**. Curiously, however, an apparently equal mixture of the triply-bridged (D_{3h}) and the singly-bridged (C_{2v}) is produced (Figure 32). This would seem to indicate that there are two competing pathways through which CO can attack **3** and **4**. If this were merely the result of re-formation of **1** and its rearrangement, the energetically favored D_{3h} structure should predominate. However, we do not have enough data to make any reasonable guess as to what is happening in this case.

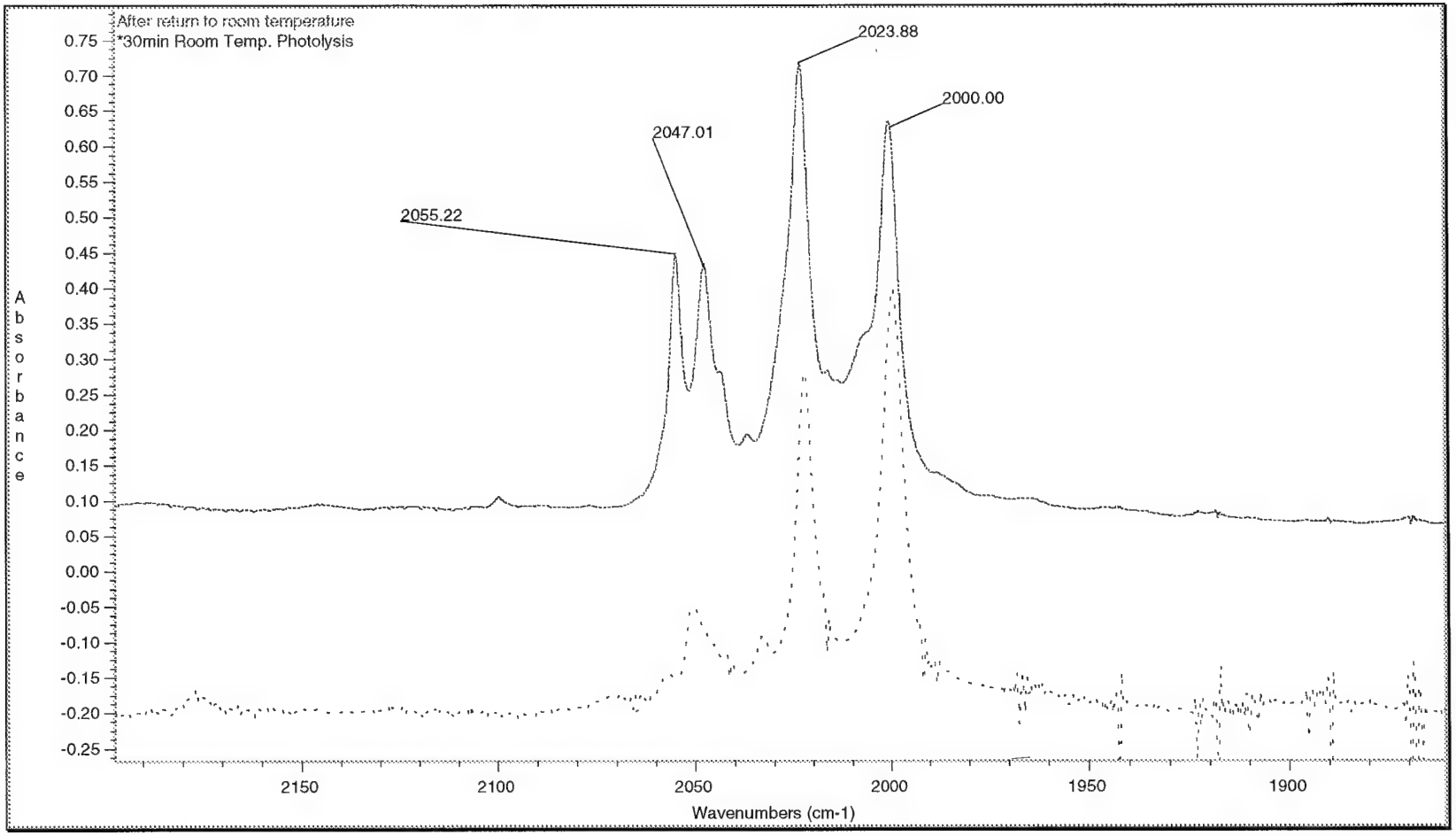

Figure 30 - Infrared Spectra - Comparison of Soft-Matrix(solid line) and Room-Temperature (dashed line) Photolysis

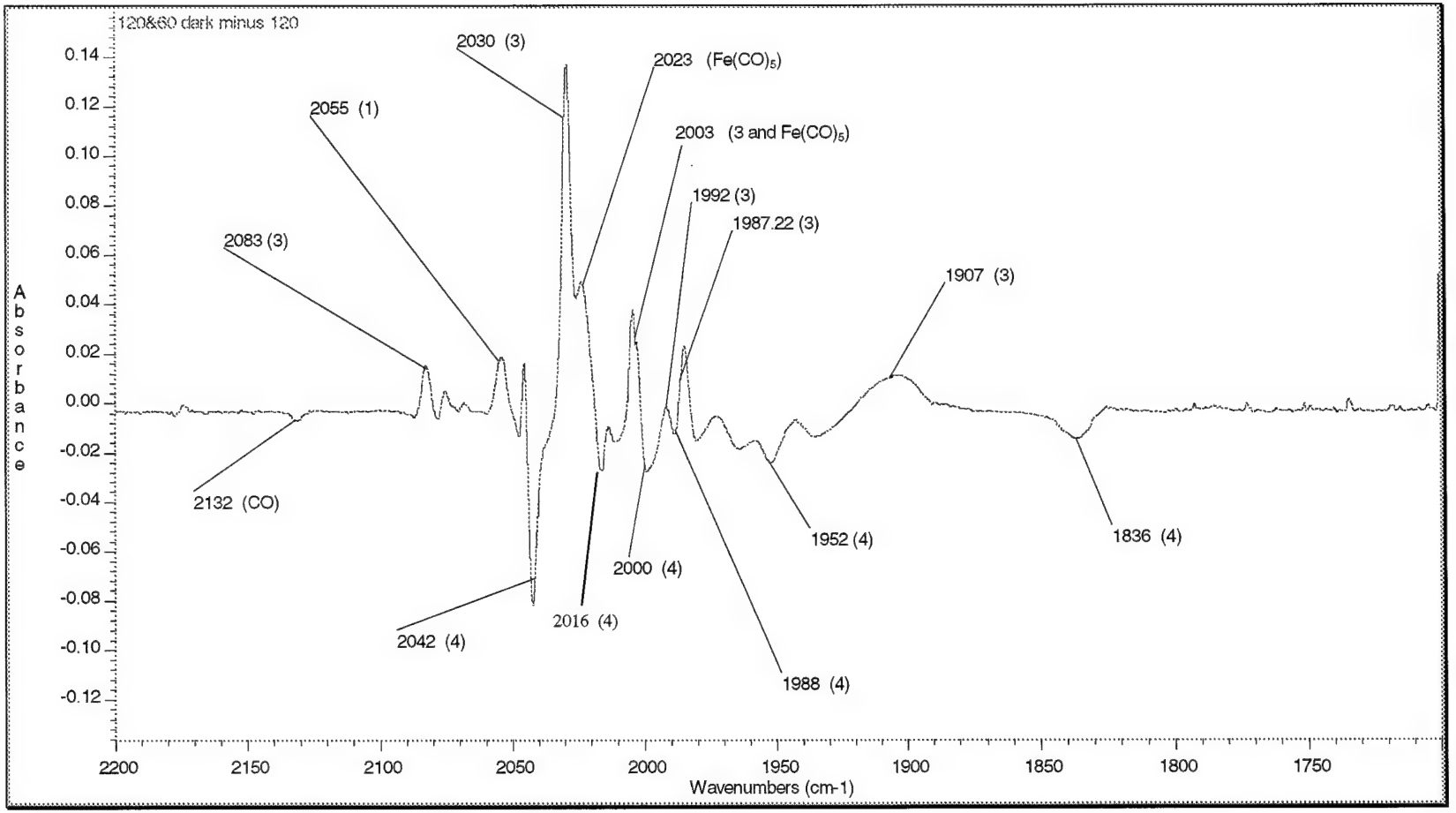

*Figure 31 - Infrared Spectrum of Cold Back-Reaction of **4** and CO, Numbers in Parentheses Indicate Species as Referenced in the Text*

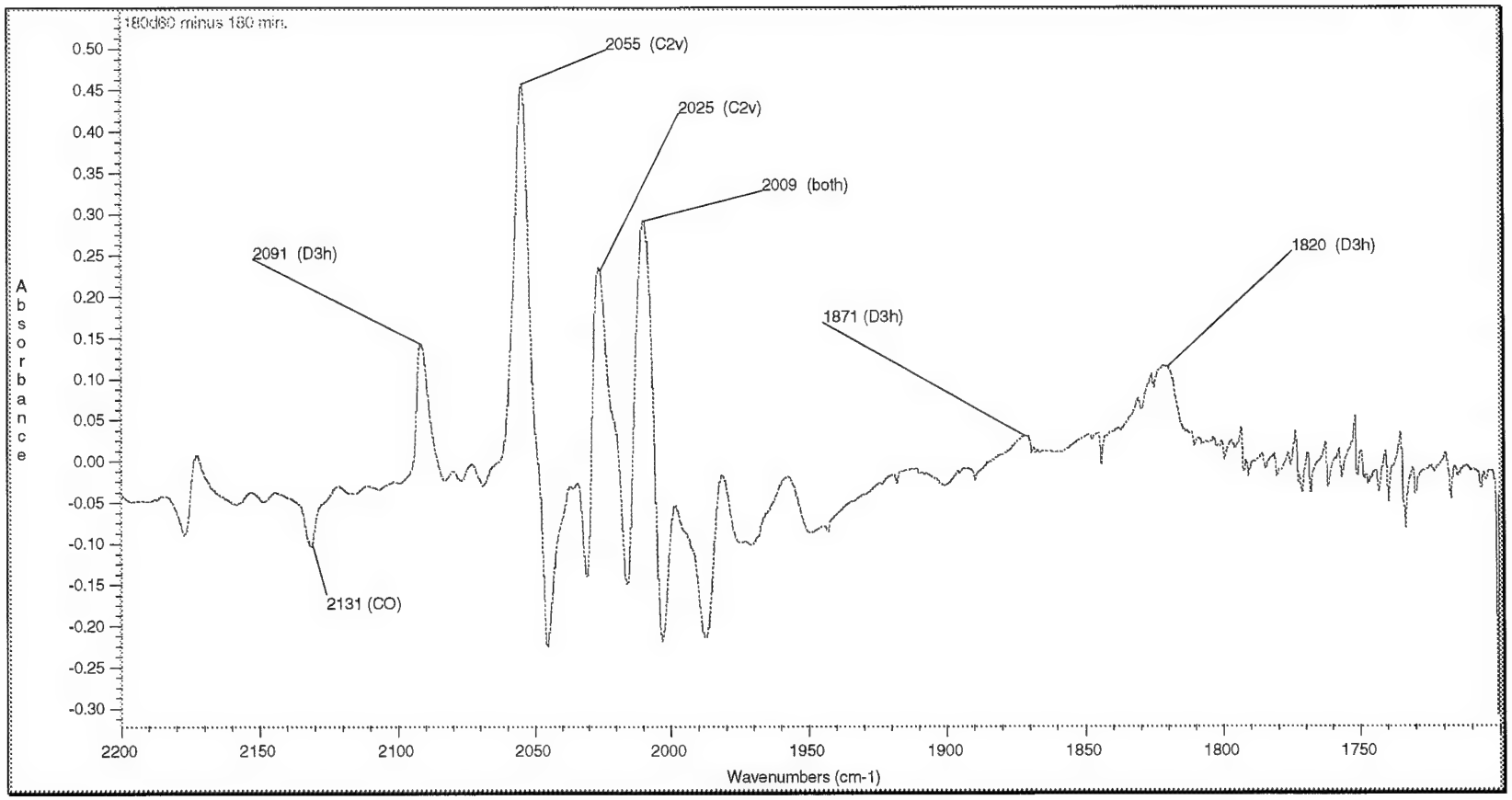

*Figure 32 - Infrared Spectrum of Thermal Back-reaction of **4** with CO, After Warming to 140 K: Marked Peaks are Assigned to **1**, with Indication of Appropriate Symmetry.*

Conclusions

Although it appears to be a simple molecule, $Fe_2(CO)_8(\mu\text{–}CH_2)$ has proven an interesting and challenging study in metal-carbonyl photochemistry. From the data presented here, irradiation of **1** with high-intensity UV/visible light promotes the formation of both single and double CO-loss products. The initial photo-product, **3,** has no bridging carbonyls and is apparently an unbalanced 16/18-electron complex. The μ-CH_2 ligand remains in place during formation of **3**, and most assuredly has a stabilizing effect on the molecule by at least partially equalizing the electron distribution on the two iron atoms. Product **3** may also be stablized by forming a *solvento* complex with 3-MP, much as $Mn_2(CO)_{10}$ is known to do. The second photo-product, **4**, is at least a doubly, and possibly a triply-bonded system. The methylene bridge apparently stays intact in this species as well, and there is at least one bridging CO. Species **4** back-reacts with CO at low temperatures (~100 K) to re-form **3**, and at higher temperatures (~140 K) to give approximately equimolar concentrations of both the C_{2v} and D_{3h} forms of **1**. This information is summarized in Figure 33.

Future Directions

There are certainly many questions which remain about this "simple" molecule. What are the *actual* structures of the CO-loss products? Why doesn't the initial photo-product contain a bridging carbonyl? Why does it forsake the energetically favored triply-bridged structure in solution? These and other questions can only be answered through further experimental research and application of theoretical methods.

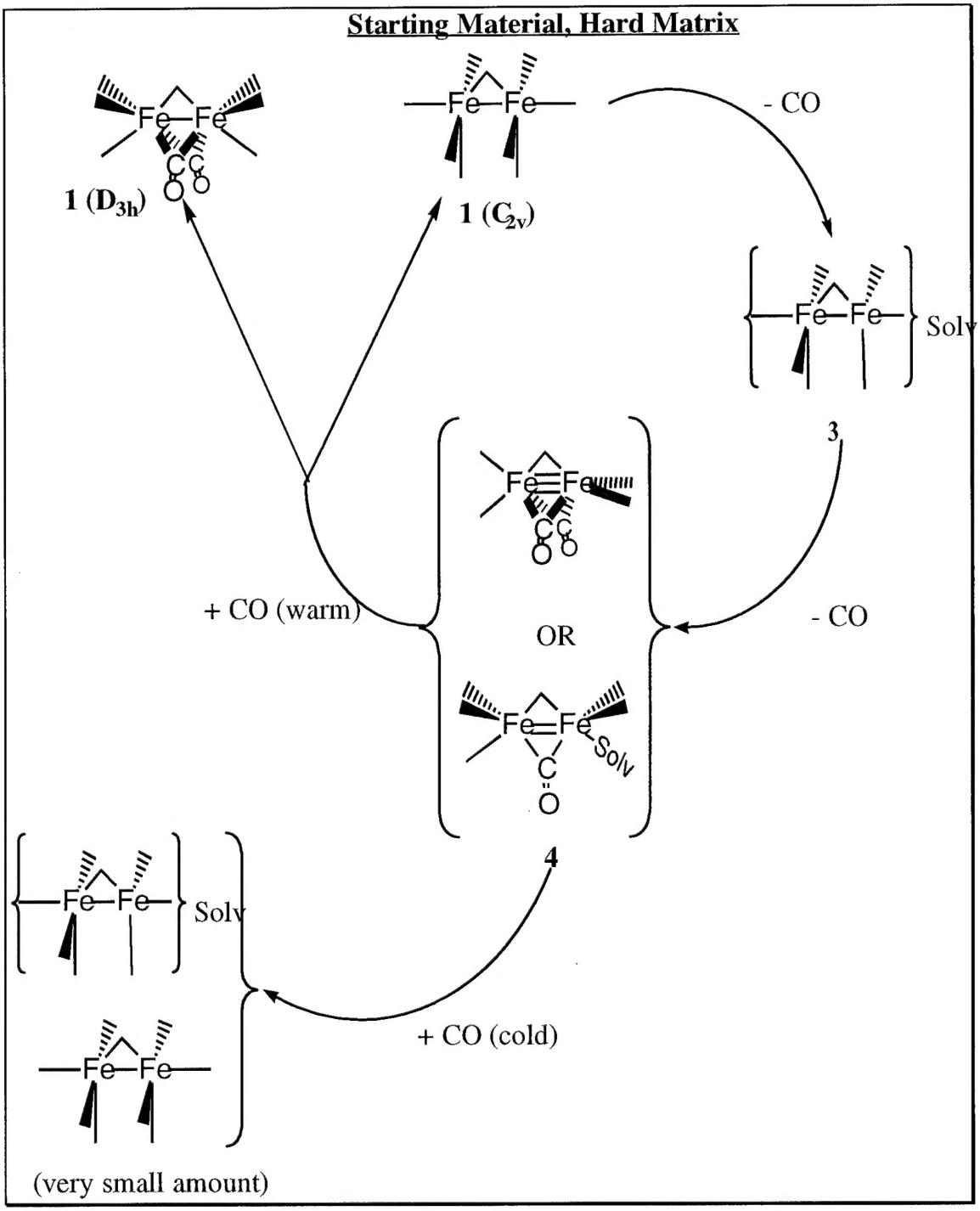

Figure 33 - Schematic Summary of Experimental Data and Conclusions

REFERENCES

"When you steal from one author, it's plagiarism; if you steal from many, it's research."

Wilson Mizner

[1] Mond, L.; Langer, C. *J. Chemical Society*, **1891**, *59*, 1090

[2] a. Kvietok, F. A.; Bursten, B. E. *Organometallics*, **1995**, *14*, 2395
b. Kvietok, F. A.; Bursten, B. E. *J. American Chemical Society*, **1995**, *116*, 9807
c. Vitale, M.; Lee, K. K. K.; Hemann, C. F.; Hille, R.; Gustafson, T. L.; Bursten, B. E. *J. American Chemical Society*, **1995**, *117*, 2286
d. Haynes, A.; Poliakoff, M.; Turner, J. J.; Bender, B. R.; Norton, J. R. *Journal of Organometallic Chemistry*, **1990**, *383*, 497
e. Poliakoff, M.; Turner, J. J. *J. Chemical Society (A)*, **1971**, 2403

[3] Herrmann, W. A. Advances in Organometallic Chemistry, **1982**, *20*, 159

[4] Mirkin, C. A.; Wrighton, M. S. *J. American Chemical Society*, **1990**, *112(23)*, 8596

[5] Vites, J.; Fehlner, T. P. *Journal of Electron Spectroscopy and Related Phenomena*, **1981**, *24*, 215

[6] Diana, E.; Gambino, O.; Rossetti, R.; Stanghellini, P. L.; Albiez, T.; Bernhardt, W.; Vahrenkamp, H. *Spectrochimica Acta*, **1993**, *49A(9)*, 1247

[7] Rosa, A.; Baerends, E. J. *New Journal of Chemistry*, **1991**, *15*, 815

[8] Moss, J. R.; Graham, W. A. G. *Chemical Communications*, **1970**, 835

[9] Motyl, K. M.; Norton, J. R.; Schauer, C. K.; Anderson, O. P. *J. American Chemical Society,* **1982**, *104*, 7325

[10] Cotton, F. A.; Lahuerta, P. *Inorganic Chemistry*, **1975**, *14*, 116

[11] Cotton, F. A.; Kolb, J. R.; Stults, B. R. *Inorg. Chimica Acta*, **1975**, *15*, 239

[12] Braterman, P. S.; Wallace, W. J. *J. Organometallic Chemistry*, **1971**, *30*, C17

[13] Sumner, C. E.; Riley, P. E.; Davis, R. E.; Pettit, R. *J. American Chemical Society*, **1980**, *102*, 1752

[14] Meyer, B. B.; Riley, P. E.; Davis, R. E. *Inorganic Chemistry*, **1982**, *20*, 3024

[15] Xiang, S.; Chen, H.; Eyermann, C. J.; Jolly, W. L.; Smit, S. P.; Theopold, K. H.;Bergman, R. G.; Herrmann, W. A.; Pettit, R. *Organometallics*, **1982**, *1*, 1200

[16] Mirkin, C. A.; Lu, K. L.; Snead, T. E.; Young, B. A.; Geoffroy, G. L.; Rheingold, A. L.; Haggerty, B. S. *J. American Chemical Society*, **1991**, *113(10)*, 3800

[17] Mirkin, C. A.; Geoffroy, G. L.; Macklin, P. D.; Rheingold, A. L. *Inorg. Chimica Acta*, **1990**, *170(1)*, 11

[18] Keng, R. S.; Lin, Y. C. *Organometallics*, **1990**, *9(1)*, 289

[19] Jeffery, J. C.; Parrott, M. J.; Stone, F. G. A. *J. Chemical Society, Dalton Transactions*, **1988,** *12*, 3017

[20] Mirkin, C. A.; Lu, K. L.; Geoffroy, G. L.; Rheingold, A. L.; Staley, D. L. *J. American Chemical Society*, **1989**, *111(18)*, 7279

[21] Zhou, Z.; Gao, J.; Fu, J.; Wang, H.; Li, Y; Tsai, K. R. *Xiamen Daxue Xuebao, Ziran Kexueban*, **1990**, *29(3)*, 286

[22] Zhou, Z.; Gao, J.; Wang, H.; Li, Y; Tsai, K. R *Fenzi Cuahua*, **1990**, *4(4)*, 257

[23] Denise, B.; Navarre, D.; Rudler, H.; Daran, J. C. *J. Organometallic Chemistry*, **1989**, *375(2)*, 273

[24] Navarre, D.; Parlier, A.; Rudler, H.; Daran, J. C. *J. Organometallic Chemistry*, **1987**, *322(1)*, 103

[25] Denise, B.; Navarre, D.; Rudler, H. *Organometallic Chemistry*, **1987**, *326(2)*, C83

[26] source of data: *Science Citation Index*

[27] Bigot, B; Delbecq, F. *Organometallics*, **1987**, *6*, 172

[28] Sumner, C. E.; Collier, J. A.; Pettit, R. *Organometallics*, **1982**, *1*, 1350

[29] Ling, A. C.; Willard, J. E. *The Journal of Physical Chemistry*, **1968**, *72(6)*,1918

[30] Chang, S; Kafafi, Z. H.; Whitmire, K. H.; Billups, W. E.; Margrave, J. L. *Inorganic Chemistry*, **1986**, *25*, 4530

[31] Pope, K. R.; Wrighton, M. S. *Inorganic Chemistry*, **1985**, *24,* 2792

[32] Jones, L. H.; McDowell, R. S.; Goldblatt, M.; Swanson, B. J. *J. Chemical Physics*, **1952**, *57*, 2050

[33] Zhang S.; Zhang, H.; Brown, T. L. *Organometallics*, **1992**, *11(12)*, 3929